GNGA: Recent Progress and Open Problems for Semilinear Elliptic PDE

John M. Neuberger

ABSTRACT. This article is a survey of successful numerical experiments which use variants of the Gradient Newton Galerkin Algorithm of Neuberger & Swift, together with a list of open problems and conjectures in semilinear elliptic PDE. The application is primarily to problems of the form $\Delta u + f(u) = 0$ on regions $\Omega \subset \mathbf{R}^2$ with zero Dirichlet boundary condition. By characterizing solutions to the PDE as critical points of an "action" functional, we consider Newton's method on the gradient of that functional. We use a Galerkin expansion, in eigenfunctions of the Laplacian, to find solutions of arbitrary Morse index. For general regions, generating this basis is one of the more computationally challenging portions of the algorithm. We often take $f'(0)$ to be a parameter, and analyze the resulting bifurcations. We also consider a one-parameter family of regions, where we then have two free bifurcation parameters. If the region or the nonlinearity has symmetry, it is often advantageous to use this information. We also report on several new numerical results and discuss related conjectures and on-going experiments.

1. Semilinear Elliptic BVP.

The Gradient Newton Galerkin Algorithm (GNGA, see [**36**]) is a general method for finding approximations of critical points of a functional. Given a Hilbert space H and a C^2 functional $J : H \to \mathbf{R}$, we work in a sufficiently large M-dimensional subspace $G \subset H$ and iteratively seek a function $u \in G$ so that the projection $P_G \nabla J(u) = 0$. For many of the semilinear elliptic Dirichlet problems that are our frequent objects of interest, it is reasonable to take $G = \text{span}\{\psi_i\}_{i=1,\ldots,M}$, where $\{\psi_i\}_{i\in\mathbf{N}}$ are the eigenfunctions of $-\Delta$ with zero Dirichlet boundary condition in Ω, and

$$0 < \lambda_1 < \lambda_2 \leq \lambda_3 \leq \cdots \to \infty \tag{1.1}$$

1991 *Mathematics Subject Classification.* Primary 35A15; Secondary 65K10.

Key words and phrases. GNGA, Variational, Bifurcation, Symmetry, Sign-Changing Solutions, Elliptic PDE.

Partially supported by NSF DMS Grants 0074326 and 0124121.

are the corresponding eigenvalues. In this case we assume that the eigenfunctions are normal in $L_2 = L_2(\Omega)$ and of course orthogonal in both the Sobolev space $H = H_0^{1,2}(\Omega)$ and in L_2, with inner products

$$\langle u, v \rangle_H = \int_\Omega \nabla u \cdot \nabla v \quad \text{and} \quad \langle u, v \rangle_2 = \int_\Omega u \; v$$

respectively (see [**1**], [**24**], or [**42**]). It is a chief goal of ours to demonstrate the importance of these eigenfunctions to the theory and numerical solution of related nonlinear elliptic equations.

Our interest in variational methods for nonlinear elliptic boundary value problems (BVP) began with [**8**], where we proved the existence of a third nontrivial solution to a superlinear Dirichlet problem of the form

$$\begin{cases} \Delta u + f(u) = 0 & \text{in } \Omega \\ u = 0 & \text{on } \partial\Omega, \end{cases} \tag{1.2}$$

where among other hypotheses, we have $f(0) = 0$ and $f'(0) < \lambda_1$. This solution, if nondegenerate, is shown to be of Morse index (MI) 2 (see [**33**]). The techniques of proofs were natural extensions of the Mountain Pass Lemma (see [**2**]), and were similarly constructive. Recently, we extended this result in [**11**] to the case where $f'(0) < \lambda_2$. Similarly to the Mountain Pass Algorithm (MPA) of [**13**], we were able to develop the so-called Modified Mountain Pass Algorithm (MMPA) (see [**34**]) for approximating the new higher MI solution through a gradient descent method with two constraints. The proof in [**8**] and the MMPA were suitably modified in [**35**] to handle a slightly different non-linearity allowing $f(0) \neq 0$ where the variational structure is more complex than the frequently studied "Nehari Manifold". In [**15**], our steepest descent techniques are further modified to realize the Lyapunov-Schmidt reductions found in [**9**] and [**10**], where asymptotically linear problems are considered. In [**17**], we use both the MMPA and numerical high-linking methods (see [**16**]) together with gradient flow invariant sets to take advantage of symmetries of Ω to approximate solutions with MI greater than 2.

In seeking a general method to find solutions of MI greater than 2, we take advantage of the minimax nature inherent to Newton's Method in order to find saddle point type critical points. In [**36**], we developed the GNGA for exactly this purpose, and were able to describe in a fairly complete way all of the solutions of reasonable MI to a standard class of superlinear Dirichlet problems on the square. For the PDE (1.2) on a square region $\Omega = (0,1) \times (0,1)$, it is well-known that the (doubly indexed) eigenvalues and eigenfunctions of $-\Delta$ are

$$\lambda_{m,n} = (m^2 + n^2)\,\pi^2 \text{ and } \psi_{m,n} = 2\sin(m\pi x)\sin(n\pi y), \tag{1.3}$$

where m and n range over all positive integers. We featured primarily the nonlinearity $f(u) = \lambda u + u^3$, and were thus able to analyze the possible types of symmetry on all of the branches bifurcating from the trivial branch at the first 6 eigenvalues of the Laplacian, as well as secondary and tertiary

bifurcations off of those branches. In [**7**], we performed analogous experiments when Ω was a disk in $\mathbf{R}^2$, using the well known basis generated from Bessel functions in that case. In [**21**], we began an ambitious effort to understand the basins of attraction for Newton's Method in general, and the GNGA for our semilinear problems in particular. One could see this effort as an attempt to generalize the finite dimensional result in [**43**] to the significantly more complicated infinite dimensional case arising from the variational study of semilinear elliptic PDE. Efforts along these lines are still on-going. We are attempting to relate these experiments to the well known Lazer-Mckenna conjecture and subsequent Dancer counterexample (see [**29**] and [**18**]). In [**39**], we apply GNGA to systems of nonlinear elliptic BVP. In particular, we are able to approximate a triple junction solution to a vector equation of Ginzburg-Landau type (see also [**22**]). We are interested in and see the potential for applying our general methods to more complicated equations from physics, such as the full Ginzburg-Landau and Monge-Ampere equations (see [**42**], and [**4**]).

Our current efforts have focused on generating eigenfunctions of the Laplacian for general regions $\Omega \subset \mathbf{R}^2$ and then applying GNGA for (1.2) on that region. We present recent results for two interesting cases. In the first, we let $\Omega = \Omega_d$ be a family of Bunimovich stadia (see [**25**], [**45**], and [**6**]). In this case, the parameter d (radii of the end cap semicircles) is treated like a second bifurcation parameter. We observe the persistence of the well-known eigenvalue crossings and avoided crossings from the linear to the nonlinear case. Most recently, we considered the case where Ω is the Koch Snowflake. After first reproducing (and possibly improving upon) the approximations to the linear problem found in [**27**], we studied the nonlinear problem (1.2). Our focus here is on the symmetry of solutions, where we once again find guidance for the nonlinear problem by first understanding what happens in the linear case. These experiments rely heavily on the package ARPACK, an implementation of the Arnoldi process called the Implicitly Restarted Arnoldi Method, most useful in finding eigenvalues and eigenvectors to very large sparse matrices. At the time of this writing, we are porting both linear and nonlinear code to work in a parallel environment on a Linux cluster.

In Section 2 we will present the general GNGA algorithm, define precisely the nonlinearities for a class of semilinear elliptic BVP, and describe the variational framework for studying this class. Furthermore, we will provide some details for implementing the GNGA for these types of nonlinear PDE. In order to make the point of the generality of the numerical method, we also include a very simple ODE example where a basis other than eigenfunctions is used. In Section 3 we provide a brief historical overview of the constrained steepest descent methods (MPA, MMPA) used to find MI 1 and MI 2 solutions of problems of a similar type. In Section 4, we outline previous results where the GNGA was applied to BVP where the region Ω was a square or a disk. Section 5 contains an application to a system of PDE,

with discussion of the applicability of the method to various scientific applications such as the full Ginzburg-Landau equation. Section 6 contains brief previews of several new results, where the basis of eigenfunctions for nonstandard regions is generated in order to further illuminate the relationship between linear and nonlinear problems. Section 7 contains several historical conjectures, some new conjectures, and describes ongoing experiments designed to further understanding of these conjectures. In Section 8, we list a number of open problems, as yet unperformed numerical experiments, and new ideas. Section 9 is the conclusion of this article.

2. GNGA and Variational Problems.

Suppose that one wants to find critical points of a C^2 functional $J : H \to \mathbf{R}$, where H is some Hilbert space. If one has good reason to believe that some of the critical points of interest lie almost entirely in an M-dimensional subspace $G \subset H$, then it should be fruitful to seek functions $u \in G$ so that the orthogonal projections $P_G \nabla J(u)$ are nearly zero. Let $G = \text{span}\{\psi_i\}_{i=1,\ldots,M}$ be such a subspace, where it is assumed that the ψ are orthogonal and suitably normalized. We use the notations $J(u) = J(\sum a_i \psi_i) = \hat{J}(a)$ interchangeably. In its most general form, we have damped Newton's Method with stepsize δ:

ALGORITHM 2.1. GNGA

(1) Choose initial coefficients $a = a^0 = \{a_k\}_{k=1}^M$, set $u = u^0 = \sum a_k \psi_k$, and set $n = 0$.
(2) Loop
   (a) Calculate $g = g^{n+1} = (J'(u)(\psi_k))_{k=1}^M \in \mathbf{R}^M$ (gradient vector).
   (b) Calculate $A = A^{n+1} = (J''(u)(\psi_j, \psi_k))_{j,k=1}^M$ (Hessian matrix).
   (c) Compute $\chi = \chi^{n+1} = A^{-1} g$ by computing inverse or pseudoinverse, solving system, or implementing least squares.
   (d) Set $a = a^{n+1} = a^n - \delta\chi$ and update $u = u^{n+1} = \sum a_k \psi_k$.
   (e) Increment loop counter n.
   (f) Calculate $\text{sig}(A(a))$ and $\hat{J}(a) = J(u)$ if desired.
   (g) Calculate approximation $\sqrt{g \cdot g}$ of $||\nabla J(u)||$; STOP if sufficiently small.

If the process converges to a nondegenerate saddle point u, then we expect that $\text{sig}(A(a^n))) := \{\text{number of negative eigenvalues of } A(a^n)\}$ to equal the MI of the critical point for n sufficiently large. The proper function spaces for semilinear elliptic BVP and other critical point problems are of course of paramount importance in both analytical and numerical investigations.

In the following simple ODE example, we take G to be spanned by the first M Legendre polynomials and $J(u) = \frac{1}{2}\int_{-1}^{1}((u+1)' - (u+1))^2\,dx = \frac{1}{2}\int_{-1}^{1}(u' - u - 1)^2\,dx$. Naturally, we are interested in global minima of J, satisfying the fundamental ODE $u' = u$. This simple type of problem

is treated at length in [**42**], where the more obvious technique of steepest descent (in the proper Sobolev space) is used; we present the example here only to demonstrate the generality of GNGA. Let $\{\psi_k\}$ be the set of Legendre polynomials in $L_2(\Omega)$ with $\Omega = (-1, 1)$, normalized if desired. For our example, let $M = 4$ so that

$$G = \text{span}\{\ 1.2247x, -0.7905 + 2.3717x^2, -2.8062x + 4.6770x^3, \\ 0.7954 - 7.9549x^2 + 9.2807x^4\}.$$

Since J is quadratic and hence $\nabla J(u)$ is linear, GNGA converges in one iteration to a nearby solution:

(1) Set $a = (0, 0, 0, 0)$ (for example) and form $u = a_1\psi_1 + \cdots + a_4\psi_4$.
(2) Loop (one iteration suffices)
  (a) Calculate $g_k = J'(u)(\psi_k) = \int_{-1}^{1}(u' - u - 1)(\psi_k' - \psi_k)\,dx$, $k = 1, \ldots, 4$.
  (b) Calculate $h_{j,k} = J'(u)(\psi_j, \psi_k) = \int_{-1}^{1}(\psi_j' - \psi_j)(\psi_k' - \psi_k)\,dx$, $j, k = 1, \ldots, 4$.
  (c) Compute χ satisfying $h\chi = g$.
  (d) Set $a = a - \chi$ and update $u = a_1\psi_1 + \cdots + a_4\psi_4$.
(3) Output a, $u + 1$, and $\sqrt{g \cdot g} = P_G\nabla J(u)$.

The above calculation yields a scalar multiple (solutions are not unique) of

$$u = 1 + 0.9962x + 0.4989x^2 + 0.1788x^3 + 0.04402x^4,$$

which is exactly $P_G y$ for an exact solution $y = e^x$, with $||y-u||_2 = 0.0007534$. Figure 1 shows plots for this example. If the above example is too obvious,

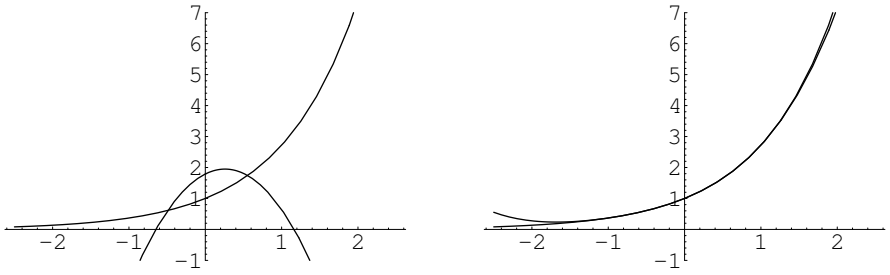

FIGURE 1. The graph on the left is of an initial guess and the 4th degree Taylor polynomial approximation of an exact solution $y = e^x$. The graph on the right compares the Taylor approximation to the function $u = P_G y$ obtained via the Newton iteration step.

we tested the method in a similar fashion on initial value problems such as $y' = 1 + y^2$, $y' = -xy$, and $(y')^2 + y^2 = 4$, where more than one iteration is required.

We now devote our attention to (1.2). Let $F(u) = \int_0^u f(s)\,ds$ for all $u \in \mathbf{R}$ define the primitive of f. We then define the action functional $J : H \to \mathbf{R}$ by

$$J(u) = \int_\Omega \left\{ \frac{1}{2}|\nabla u|^2 - F(u) \right\} dx. \tag{2.1}$$

We will make assumptions on f so that J is well defined and of class C^2 on H. Taking λ_i and ψ_i as in (1.1) and integrating by parts, a calculation shows that

$$J'(u)(\psi_i) = \int_\Omega \{\nabla u \cdot \nabla \psi_i - f(u)\,\psi_i\}\,dx = a_i\lambda_i - \int_\Omega f(u)\,v\,dx \tag{2.2}$$

and

$$J''(u)(\psi_i, \psi_j) = \int_\Omega \{\nabla \psi_i \cdot \nabla \psi_j - f'(u)\,\psi_i\,\psi_j\}\,dx = \lambda_i\delta_{ij} - \int_\Omega f(u)\,\psi_i\,\psi_j\}\,dx, \tag{2.3}$$

where δ_{ij} is the Kronecker delta function. In this case, note that there is no need for numerical integration when implementing Algorithm 2.1. This information is encoded in the solutions (eigenpairs) of the linear problem. It is well known that critical points of J are in fact solutions to (1.2) (see for example [**46**] and [**24**]). For the types of nonlinearities f we will consider, most if not all nontrivial solutions are saddle points of J. Roughly speaking, the Morse index is the number of linearly independent directions in function space in which J "curves down" at a (nondegenerate) solution u. This is the number of negative eigenvalues of the Hessian $D^2J(u)$, and for M and n in Algorithm 2.1 sufficiently large, also equal (one hopes) to $\mathrm{sig}(A)$. See [**33**] for more information about Morse index (MI).

We now give a precise statement of the hypothesis on the nonlinearity f that leads to existence and nodal structure theorems as well as the numerical approximation of solutions (see for example [**2**], [**8**], [**34**], [**9**], [**10**], [**11**], [**36**], [**47**], and [**48**]). In particular, we take $f \in C^1(\mathbf{R}, \mathbf{R})$ such that $f(0) = 0$. In general we assume that $f'(0) < \lambda_1$. This is necessary in order to find one-sign solutions. In [**11**] we assume that $f'(0) < \lambda_2$ and are able to prove the existence of a sign-changing exactly-once solution; we also demonstrated the existence of a solution which changes sign at most k times when $f'(0) < \lambda_k$.

We assume that there exist constants $A > 0$ and $p \in (1, \frac{N+2}{N-2})$ such that $|f'(u)| \le A(|u|^{p-1} + 1)$ for all $u \in \mathbf{R}$. It follows that f is *subcritical*, i.e., there exists $B > 0$ such that $|f(u)| \le B(|u|^p + 1)$. For $N = 1$ this condition is omitted, while for $N = 2$ it suffices to have $p \in (1, \infty)$ (see [**46**]). Also, we assume that there exists $m \in (0, 1)$ such that

$$\frac{m}{2} f(u)u \ge F(u), \tag{2.4}$$

(in fact this need only hold for $|u| > \rho$ for some $\rho > 0$), and that f is *superlinear*, i.e.,

$$\lim_{|u|\to\infty} \frac{f(u)}{u} = \infty. \tag{2.5}$$

Finally, we make the assumption that f satisfies

$$f'(u) > \frac{f(u)}{u} \quad \text{for } u \neq 0. \tag{2.6}$$

For convenience, we will call (1.2) with all of the above conditions on f "the superlinear problem". Recall that subcritical growth and the Sobolev Embedding Theorem (see [**1**]) imply that H is compactly embedded into L_{p+1}, which in turn shows that J is well defined on all of H. Under this hypothesis, J is in fact twice differentiable on H (see [**46**]).

In [**8**], the Mountain Pass argument used in [**2**] to find one-sign solutions to the superlinear problem was extended to find a sign-changing solution. Rather than one constraint, the theorem uses two constraints to find a MI 2 (if nondegenerate) solution to (1.2) using a subset of the well known Nehari manifold $S = \{u \in H \setminus \{0\} : J'(u)(u) = 0\}$:

THEOREM 2.1 (The CCN Theorem [**8**]). *If $f'(0) < \lambda_1$, then the superlinear problem* (1.2) *has at least three nontrivial solutions: $\omega_1 > 0$ in Ω, $\omega_2 < 0$ in Ω, and ω_3. The function ω_3 changes sign exactly once in Ω, i.e., $(\omega_3)^{-1}(\mathbf{R} \setminus \{0\})$ has exactly two connected components. If nondegenerate, the one-sign solutions are Morse index (MI) 1 critical points of J, and the sign-changing solution has MI 2. Furthermore,*

$$J(\omega_3) \geq J(\omega_1) + J(\omega_2).$$

For convenience, we call ω_3 the CCN solution. In this $f'(0) < \lambda_1$ superlinear case, the trivial solution $u = 0$ has MI 0 and is the only local minimum of J. All other critical points (solutions to (1.2)) are saddle points. With $u_+ = \max_\Omega\{u, 0\}$ and $u_- = \min_\Omega\{u, 0\}$, we can define the subset

$$S_1 = \{u \in S : u_+ \in S, u_- \in S\}, \tag{2.7}$$

which allows us to restate the CCN Theorem:

THEOREM 2.2 (CCN). *For the superlinear problem, given $f'(0) < \lambda_1$ there exist solutions $\omega_1 > 0$, $\omega_2 < 0$, and ω_3 which changes sign exactly once, where ω_1 and ω_2 are local (possibly global) minimizers of $J|_S$ and $J(\omega_3) = \min_{S_1} J$.*

In [**11**] we find that the MI 2 CCN solution persists when $f'(0) \in [\lambda_1, \lambda_2)$, which suggests that one let $\lambda = f'(0)$ vary as a bifurcation parameter. Using GNGA, we are able to accurately and thoroughly construct the portion of the bifurcation diagram corresponding to the first few eigenvalues (how few essentially depends only on the choice of M for the dimension of G). Ultimately, we seek to prove the existence and describe the nodal structure

of all solutions to the superlinear problem (and indeed PDE (1.2) with other types of nonlinearities).

Although theory tells us that the so-called weak solutions in H are in fact in C^2, it is necessary to use the Hilbert space H as the domain of the functional J in order to find existence proofs. When considering numerical steepest descent methods, it is essential that one not use the poorly performing (and only densely defined) L_2 gradient (see [**42**]). We will be restricting our approximations to the finite dimensional subspace G of L_2, which consists of twice continuously differentiable functions. In this case, we may use the L_2 gradient $\nabla_2 J(u)$ and Hessian $\mathbf{D}_2^2 J(u)$, since the Newton search direction is seen to satisfy

$$\chi = (D_H^2 J(u))^{-1} \nabla_H J(u) = (D_2^2 J(u))^{-1} \nabla_2 J(u).$$

Thus, our implementation of Algorithm 2.1 approximates the infinite dimensional Newton iteration

$$u_{k+1} = u_k - (D_H^2 J(u_k))^{-1} \nabla_H J(u_k), \tag{2.8}$$

and the corresponding continuous infinite dimensional "flow" (ODE)

$$u'(t) = -(D_H^2 J(u(t)))^{-1} \nabla_H J(u(t)). \tag{2.9}$$

As a practical matter, since $D^2 J(u)$ may be noninvertible or ill conditioned, one should consider using singular value decomposition and pseudo inverses, least squares, or a system solver which handles our possible types of singularities when computing this search direction. At nondegenerate solutions, the Hessian is nonsingular in a neighborhood of the solution and the pseudoinverse is not needed. However, we are sometimes interested in degenerate solutions, for example at bifurcation points or non-radial solutions to the PDE on a disk where there is a continuum of solutions. We have found the algorithm to be surprisingly robust even when an actual inverse is computed and used very near a singularity, an interesting phenomena worthy of future study. In many cases the corresponding zero-eigenfunction directions are nearly orthogonal to nearby gradients, and hence had little effect on the "projected gradient" (Newton) search direction.

3. Mountain Pass and Modified Mountain Pass Algorithms

Historically, the MPA found in [**13**] represents the first numerical minimax technique applied to semilinear elliptic problems, although constrained optimization was not itself a new idea. The MPA is based on the Mountain Pass Lemma and the landmark existence theorem for one-sign solutions found in [**2**]. We briefly present a version of this algorithm as applied to the superlinear problem. We also describe the MMPA (see [**34**]) which likewise was developed from the constructive proof found in [**8**]. Both algorithms are applied here to the superlinear problem; different nonlinearities may significantly change the variational structure and hence necessitate modifications.

Since under the hypothesis of Theorem 2.1 the set S is a manifold, we can use the facts that given $u \neq 0$ there exists a unique $\hat{\alpha} > 0$ such that $\hat{\alpha}u \in S$ and that $J(\hat{\alpha}u) = \max_{\alpha>0} J(\alpha u)$ to project nonzero elements of H on to S and sign-changing elements of H on to S_1. The Sobolev gradient $\nabla_H J(u) = u + z$ where $\Delta z = f(u)$ can be computed by solving a system via standard algorithms.

ALGORITHM 3.1. MPA

(1) Choose u of one sign (Typically $\pm c\psi_1$).
(2) Loop
  (a) Project u on to S by iterating $u + \sigma_1 P_u \nabla_H J(u) \to u$ (Ascent).
  (b) Solve a sparse system to compute $\nabla_H J(u) = u + (\Delta)^{-1} f(u)$.
  (c) Set $u - \sigma_2 \nabla_H J(u) \to u$ (Descent).
  (d) Stop when $||\nabla_H J(u)||_H$ is sufficiently small.

Similarly,

ALGORITHM 3.2. MMPA

(1) Choose u which changes sign exactly once (Typically $\pm c\psi_2$).
(2) Loop
  (a) Project u_+ on to S by iterating $u_+ + \sigma_1 P_{u_+} \nabla_H J(u_+) \to u_+$ (Ascent).
  (b) Project u_- on to S by iterating $u_- + \sigma_1 P_{u_-} \nabla_H J(u_-) \to u_-$ (Ascent).
  (c) Add $u = u_+ + u_- \in S_1$.
  (d) Solve a sparse system to compute $\nabla_H J(u) = u + (\Delta)^{-1} f(u)$.
  (e) Set $u - \sigma_2 \nabla_H J(u) \to u$ (Descent).
  (f) Stop when $||\nabla J(u)||_H$ is sufficiently small.

In both cases the step sizes σ_1 and σ_2 may be taken to be 1 if the initial guess is sufficiently close to a solution.

In general, the above methods will only find MI 1 and MI 2 solutions, respectively. It is easy to make guesses near higher MI solutions, and observe "instability" as iterates approach then fall away from such higher energy critical points. In [**17**] the MMPA is modified so that iterates u and corresponding gradients $\nabla_H J(u)$ are constrained to invariant subspaces corresponding to symmetry groups for a given region Ω. One simply inserts a step after the projection on to S_1 whereby u is replaced with Pu, the projection of u on to the invariant subspace. As an example, when $\Omega = (0,1) \times (0,1)$ for the superlinear problem with $f(u) = u^3$, we can find a MI 8 solution which is 90^o rotationally invariant and changes sign exactly once. In practice, this is implemented by replacing an iterate with the average of all four 90^o rotations.

So what does one do to find higher Morse index solutions? The existence of higher codimension sets analogous to S and S_1 is open. If we had such sets we would have the theory to prove the existence of many more solutions.

One scheme we have tried successfully (see [**42**]), if not efficiently, is to find global minimizers of the functional ϕ defined by

$$\phi(u) = \frac{1}{2}||\nabla_H J(u)||_2^2.$$

Obviously all critical points of J are now zeroes of the non negative functional ϕ. We suggest [**42**] as a reference for this and other steepest descent techniques. The potential exists for doing analysis on the behavior of ϕ (similar to that done on J in [**8**] and elsewhere) which might well lead to existence proofs. Since

$$\chi = (D^2 J(u))^{-1} \nabla J(u) = \sum \frac{1}{\beta_i} P_{e_i} \nabla J(u) \quad \text{with } D^2 J(u) e_i = \beta_i e_i,$$

Newton's method on the gradient can be viewed as a natural extension of the MPA and MMPA. In directions e_i where $\beta_i > 0$ (and hence J is concave up), one is doing steepest descent. Conversely, when $\beta_i < 0$, steepest ascent is performed. In this way, GNGA simulates constrained steepest descent when finding critical points of arbitrarily high MI.

4. Newton's Method and Morse Index: The Unit Square and Disk.

On regions other than those where the eigenfunctions are known in closed form there will be a substantial effort required to generate the basis, as described in Section 6. This effort will only have to be done once for each given region and eliminates the need for numerical differentiation when computing Newton search directions. However, when $\Omega = (0,1)^2$ or $B_1(0) \subset \mathbf{R}^2$, the exact basis is known in terms of sines, cosines, and/or Bessel functions. In this section we briefly describe the numerical results found in [**36**] and [**7**].

Newton's method converges very well given a good initial guess and is unpredictable given a poor initial guess. Understanding basins of attraction is difficult, interesting, and very important. Our rule of thumb for superlinear problems is to use an appropriate multiple of an eigenfunction having a prescribed nodal structure and signature. When f is odd, this works well provided the multiple is in the right ball park; we can use the numerical observation that $\lim_{\alpha \to \infty} \text{sig}(\alpha \psi_i) = \infty$ for all $i \in \mathbf{N}$ to obtain the appropriate multiplier.

When f is not so nice, solutions may have nodal structures that do not closely match that of eigenfunctions, whereby multiples of eigenfunctions may not be good starting points. Since our nonlinearity is of the form $f(u) = \lambda u + g(u)$ with $g'(0) = 0$, we can use λ as a bifurcation parameter and look for solutions which do closely resemble eigenfunctions by first starting near primary bifurcation points off of the trivial branch at λ just less than the corresponding eigenvalue. One then decrements (or increments) the bifurcation parameter to follow the branch towards the desired solution at (say) $\lambda = 0$. At each step we use the solution at the previous λ as the next initial guess. The matter is somewhat more delicate at secondary bifurcation

points. In this case we add a small linear combination of zero-eigenfunctions of $D^2J(u)$ to a nearby element of the primary branch, where u is the singular bifurcation point. The same philosophy applies for finding tertiary branches off of secondary branches. In most of our experiments, we are able to use symmetry to make intelligent initial guesses. Our continuation techniques are effective but could no doubt be refined (see for example [**31**]).

In [**36**] we additionally provide an efficient method for implementing the GNGA scheme when f is polynomial. In that case, $\hat{J}$, g, and A are themselves polynomials in a, and once various integrals are calculated, no further integration needs to be performed. In that work we also investigated numerically polynomials which did not satisfy our exact CCN superlinear hypothesis. We present here a few excerpts of the superlinear results, in particular the bifurcation diagrams constructed therein when investigating the BVP (1.2) on the square $\Omega = (0,1)\times(0,1)$ with $f(u) = \lambda u + u^3$, where λ is treated as a bifurcation parameter. In [**36**], we spend considerable effort to use the symmetry of the square to explain and analyze the expected proliferation of solutions. Figure 2 depicts the first 9 primary branches that bifurcate from the origin at $\lambda \leq \lambda_{2,3} = 13\pi^2$.

At a bifurcation from a simple eigenvalue, there is a pitchfork bifurcation that creates two solutions with the same action J. Hence one branch is observed bifurcating from $2\pi^2$ and $8\pi^2$ in Figure 2. Double eigenvalues lead to two types of bifurcation, *pure modes* and *mixed modes*. Near the bifurcation, the pure modes are asymptotically a multiple of an eigenfunction $\pm\psi_{i,j}$ or $\pm\psi_{j,i}$. The mixed modes are asymptotic to a multiple of one of the four combinations of eigenfunctions $\pm\psi_{i,j} \pm \psi_{j,i}$. Naturally the behavior is more complicated at higher multiplicity eigenvalues. Of the branches seen in Figure 2, the solutions which bifurcate from $\lambda_{1,3}$ are the most interesting. Leaving the details to [**36**], we observe in Figures 3 and 4 secondary and tertiary bifurcations off of these primary branches. The tertiary branch we found contained solutions with no symmetry whatsoever. We are confident that we completely classified and numerically found all possible types of solutions found emmenating from this double eigenvalue, although we certainly do not have existence proofs. We do not include here our tests on the convergence of our results as $N_{\max}$ increases.

In a similar but technically more challenging application, we considered in [**7**] the case where $\Omega = B_1(0) \subset \mathbf{R}^2$. The eigenvalues of $-\Delta$ with zero Dirichlet boundary values on the disk are determined by the zeroes of the various Bessel functions of the first kind. The corresponding eigenfunctions, which form an orthonormal basis, are divided into three components. The radial component is defined by

$$\psi_i = a_i J_0(\sqrt{\lambda_i^0}\, r),$$

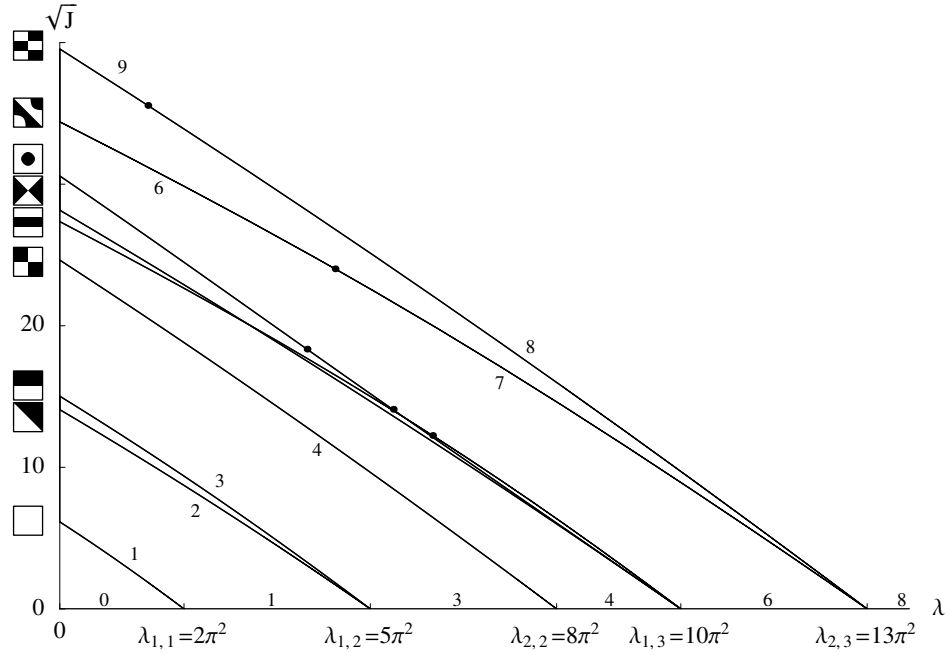

FIGURE 2. Bifurcation diagram showing $\sqrt{J}$ as a function of λ, for $f(u) = \lambda u + u^3$. Only the primary branches (the ones which bifurcate from the origin) are shown. The MI is indicated by the small numbers. The dots indicate where the MI changes at secondary bifurcations which create solutions that are not shown in this figure. More detail of the three branches that bifurcate from $\lambda_{1,3}$ is given in the next two figures. This figure is adapted from Figure 4 in [**36**], used with permission of the IJBC.

where J_0 is the Bessel Zero function, $\sqrt{\lambda_i^0}$ is the i^{th} zero of $J_0(r)$, and $a_i = \frac{1}{\sqrt{\int_\Omega J_0(\sqrt{\lambda_i^0}\, r)^2}}$. That is to say, a_i, is calculated so that $\int \psi_i^2 = 1$. The remaining two components of the orthonormal basis are the nonradial components and are given by

$$\varphi_{i,j} = b_{i,j} J_i(\sqrt{\lambda_j^i}\, r)\cos(i\theta)$$

and

$$\chi_{i,j} = b_{i,j} J_i(\sqrt{\lambda_j^i}\, r)\sin(i\theta).$$

Here J_i denotes the various Bessel functions for $i \neq 0$, $\sqrt{\lambda_j^i}$ is the j^{th} zero of the i^{th} Bessel function, and $b_{i,j}$ is calculated so that $\int \varphi_{i,j}^2 = 1$, and $\int \chi_{i,j}^2 =$

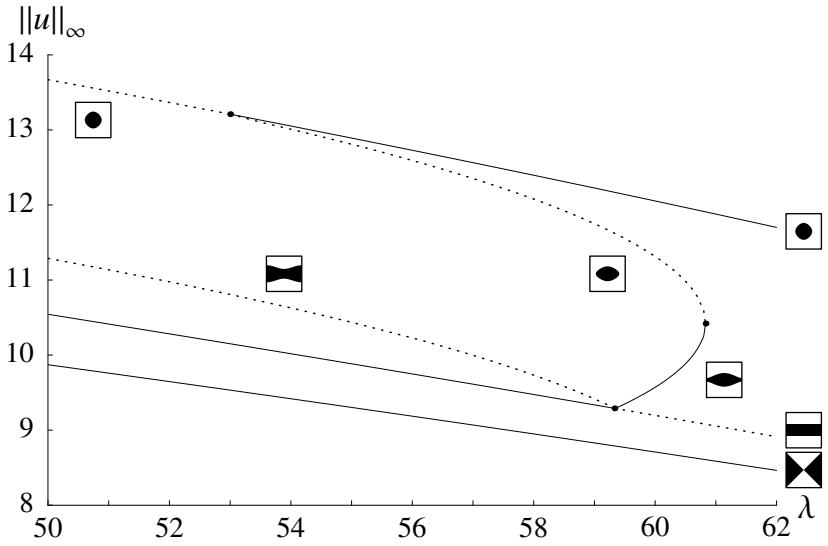

FIGURE 3. Detail of Figure 2 for the branches that bifurcate from $\lambda_{1,3}$. The supremum norm, $\|u\|_\infty$, is plotted against λ because it gives a good separation between the branches. The solutions with MI 5 are solid lines, and the solutions with MI 6 are dotted lines. This figure was computed with $N_{\max} = 9$ (81 Fourier modes). Figure adapted from Figure 5 in [**36**], with permission from the IJBC.

1. Thus, given $u \in L^2$ there exist constants $\{a_i\}$, $\{b_{i,j}\}$, and $\{c_{i,j}\}$ so that

$$u = \sum_i a_i \psi_i + \sum_i \sum_j b_{i,j} \varphi_{i,j} + \sum_i \sum_j c_{i,j} \chi_{i,j}.$$

Using this basis in exactly the same way as described above for the square, we were able to find many solutions to the nonlinear problem. In particular, we found the radial solutions guaranteed to exist by [**12**], as well as the expected nonradial ones. The symmetry can be analyzed as in [**36**], and bifurcations from the trivial branch predicted. At this time, we have not conclusively found any secondary bifurcations nor concluded that they do not exist. The matter remains open, and so we are not including a bifurcation diagram in this article. Figure 5 depicts a GNGA-approximated MI 2 CCN solution on the disk.

5. GNGA and Semilinear Systems.

In [**39**] we investigate the application of GNGA to systems of elliptic BVP. In particular, we find a triple junction solution conjectured to exist in

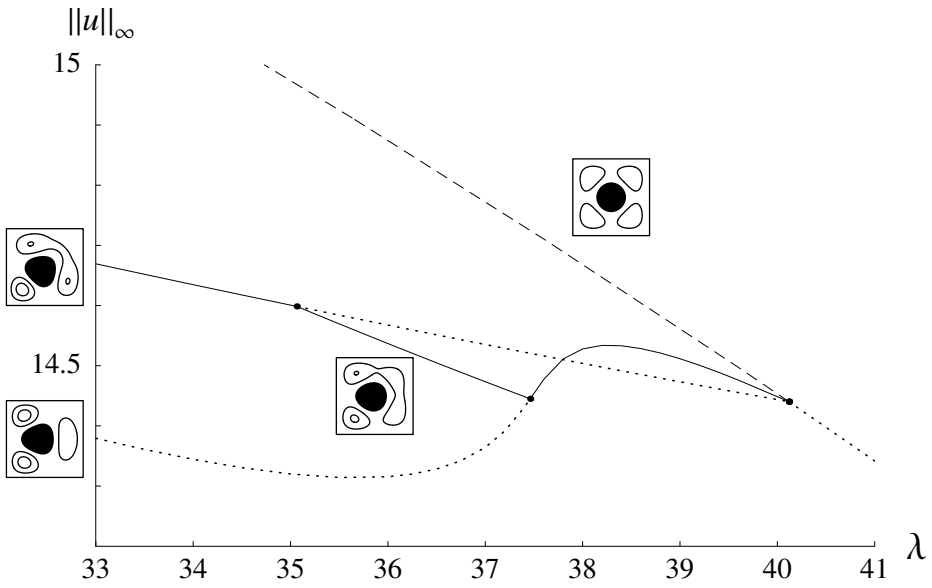

FIGURE 4. Further detail of Figure 2. The "radial" solution undergoes a bifurcation with $\mathbf{D}_4$ symmetry at $\lambda \approx 40$, creating the vertex and edge solutions. These secondary solutions in turn bifurcate, creating a branch of tertiary solutions that exist for λ in the approximate interval $[35.1, 37.5]$. These tertiary solutions have no symmetry. The Morse indices are indicated by the line type: MI 6 are dotted, MI 7 are solid, and MI 8 are dashed lines. Along with the black region, showing where $u < 0$, the contours at $u = 1/3\|u\|_\infty$ and $u = 2/3\|u\|_\infty$ are shown to better see the symmetry of the patterns. This figure was computed with $N_{\max} = 7$ (49 Fourier modes). Figure adapted from Figure 6 in [**36**], with permission from the IJBC.

[**22**] to the vector Ginzburg-Landau type problem:

$$\begin{cases} -\epsilon^2 \Delta u + \nabla W(u) = 0 \quad \text{in } \Omega \\ \qquad\qquad \dfrac{\partial u}{\partial \eta} = 0 \quad \text{on } \partial\Omega, \end{cases} \tag{5.1}$$

where $\Omega = (0,1) \times (0,1)$, $u : \Omega \to \mathbf{R}^2$, $W : \mathbf{R}^2 \to [0, \infty)$ is a triple-well potential, η is the unit outer normal to the boundary, and $\epsilon > 0$ is a parameter. The gradient in $\nabla W(u)$ is with respect to u, hence $\nabla W = (\partial W/\partial u_1, \partial W/\partial u_2)$. The triple-well potential W achieves a global minimum of zero at 3 points, and has 7 critical points in total. Figure 6 shows the contour graph of the potential that we used in our experiments.

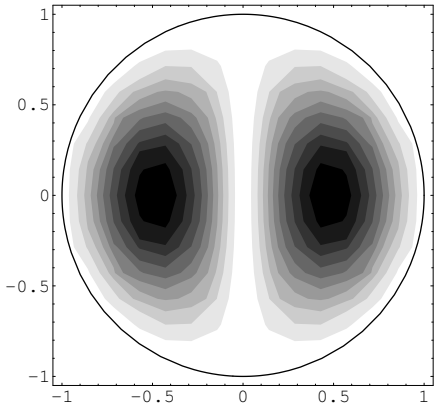

FIGURE 5. MI 2 CCN Solution on the unit disk.

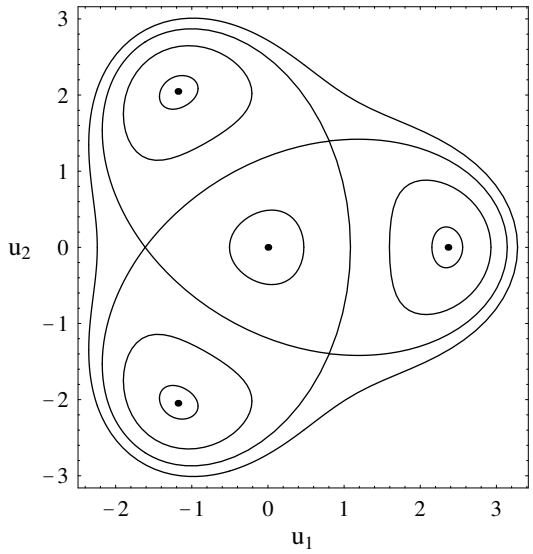

FIGURE 6. The triple-well potential W. The graph shows the minima and local maximum of W as dots, as well as the contours through the 3 saddle points and around the local extrema. Figure adapted from Figure 1 in [**39**], with permission from the IJBC.

We worked with sufficiently smooth functions $u \in L_2 \times L_2$. Since this problem is again on the square, we use known eigenfunctions similar to those found in (1.3) to form a basis for L_2, and then take a product to get a basis for $L_2 \times L_2$. Specifically, the (doubly-indexed) eigenvalues of $-\Delta$ are $\lambda_{m,n} = (m^2 + n^2)\pi^2$ and the eigenfunctions $\psi_{m,n}$ of $-\Delta$, normalized in L_2,

are given by:

$$\psi_{m,n}(x,y) = \begin{cases} 1 & \text{for } m = n = 0 \\ \sqrt{2}\cos(m\pi x)\cos(n\pi y) & \text{for } m = 0, n \neq 0 \text{ or } n = 0, m \neq 0 \\ 2\cos(m\pi x)\cos(n\pi y) & \text{for } m \neq 0 \text{ and } n \neq 0, \end{cases}$$

where m and n range over all of the nonnegative integers. It is well known that $\{\psi_{m,n}\}$ forms a basis for L_2 and $H = H^{1,2}(\Omega)$ [Adams, 1975]. We obtain a finite sub-basis (basis for a subspace) of L_2 or H by choosing a positive integer k, and including all eigenfunctions whose eigenvalues are strictly less than $\pi^2 k^2$. These eigenvalues are then ordered and singly indexed as $\lambda_1 = 0 < \lambda_2 \leq \lambda_3 \leq ... \leq \lambda_{\widetilde{M}}$. This yields a singly indexed basis, $\{\psi_i\}$, of size $\widetilde{M}$. In our experiments, typically k is an even integer ranging from $k = 8$ ($\widetilde{M} = 56$) up to $k = 18$ ($\widetilde{M} = 269$). As a rule of thumb, we trust a numerical calculation if the results are not significantly changed when the cutoff parameter k is increased by 2. We use the following Galerkin subspace of $H \times H$ and $L_2 \times L_2$:

$$G = \text{Span}\{\Psi_i\}_{i=1}^{M} := \text{Span}\left\{ \begin{pmatrix} \psi_i \\ 0 \end{pmatrix} \right\}_{i=1}^{\widetilde{M}} \bigcup \left\{ \begin{pmatrix} 0 \\ \psi_i \end{pmatrix} \right\}_{i=1}^{\widetilde{M}},$$

which is of dimension $M = 2\widetilde{M}$. The energy functional whose critical points are solutions to (5.1) is defined by

$$J_\epsilon(u) = \frac{1}{\epsilon} \int_\Omega \left(\frac{\epsilon^2}{2} |\nabla u|^2 + W(u) \right) dx\, dy. \tag{5.2}$$

A calculation shows that the directional derivative of J at u in the Ψ_j direction is

$$\begin{aligned} g_j(u) := J'(u)(\Psi_j) &= \int_\Omega \left(\epsilon \nabla u \cdot \nabla \Psi_j + \frac{1}{\epsilon} \Psi_j \cdot \nabla W(u) \right) dx\, dy \\ &= \int_\Omega \left(\epsilon \sum_{i=1}^{M} a_i \left(\nabla \Psi_i \cdot \nabla \Psi_j \right) + \frac{1}{\epsilon} \Psi_j \cdot \nabla W(u) \right) dx\, dy \\ &= \epsilon a_j \lambda_j + \frac{1}{\epsilon} \int_\Omega \Psi_j \cdot \nabla W(u)\, dx\, dy. \end{aligned}$$

Second directional derivatives can be computed similarly, whence GNGA (Algorithm 2.1) can be implemented. When u is identically a constant critical number of W, we have a trivial solution. Figure 7 depicts a diagram of solutions bifurcating off of the trivial branches corresponding to the saddle and local maxima of W, as $\epsilon \to 0$. Figure 8 shows the various types of symmetries found in such solutions. Note that for small ϵ, the solutions tend towards step functions whose piecewise constants are critical numbers of the triple well potential W. It may well be that there are alternate choices for a basis with superior behavior in approximating the near step function solutions depicted in Figure 8, as there is no longer a dominant eigenmode in the expansion for such functions.

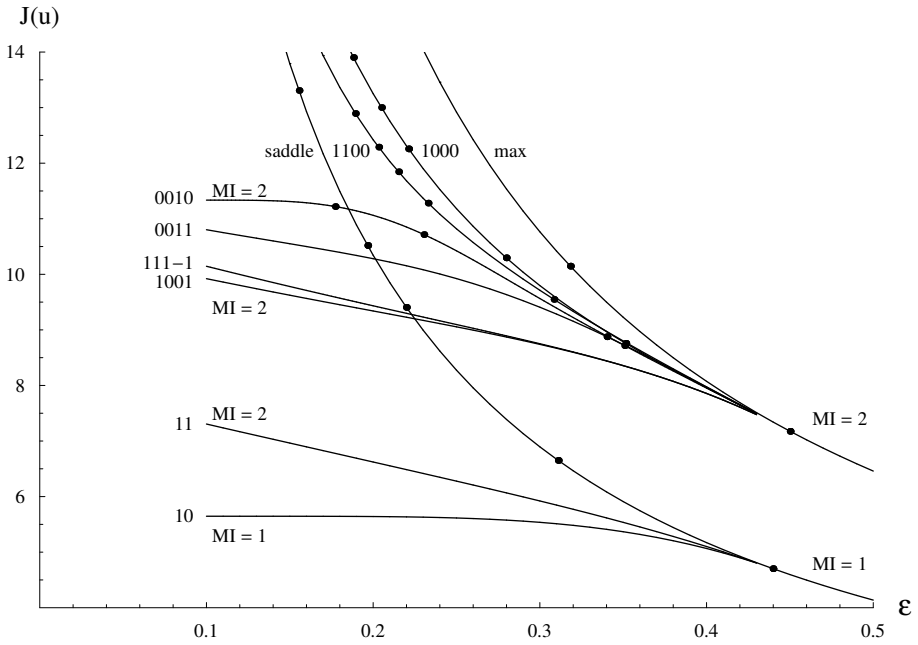

FIGURE 7. This bifurcation diagram shows the saddle solution, the maximum solution, and the solutions which bifurcate off these trivial solution branches at the first bifurcation as ϵ is decreased. The minimum solution, which is not shown, has $J = 0$ and MI 0 for all ϵ. The dots indicate a bifurcation point, where the MI changes. The lowest MI 2 secondary branch bifurcating off of the trivial maximum solution converges to the triple junction as $\epsilon \to 0$. The MI of the branches is indicated by "color"; subsequently we have preferred to identify branches by symmetry type rather than MI. Figure adapted from Figure 2 in [**39**], with permission from the IJBC.

We are also interested in the so-called full Ginzburg-Landau equation, other physical applications such as the Monge-Ampere equation, and finding a CCN-type solution for a system (see Section 8). In order to make this last problem statement precise, we present here a possible set of hypotheses to consider when looking for sign-changing solutions to superlinear systems.

We wish to generalize the hypotheses from [**8**] to the following system, in hopes that the techniques and results from that work will apply. In particular, we consider

$$\begin{cases} \Delta u + \nabla W(u) = 0 & \text{in } \Omega \\ u = 0 & \text{in } \partial\Omega, \end{cases} \tag{5.3}$$

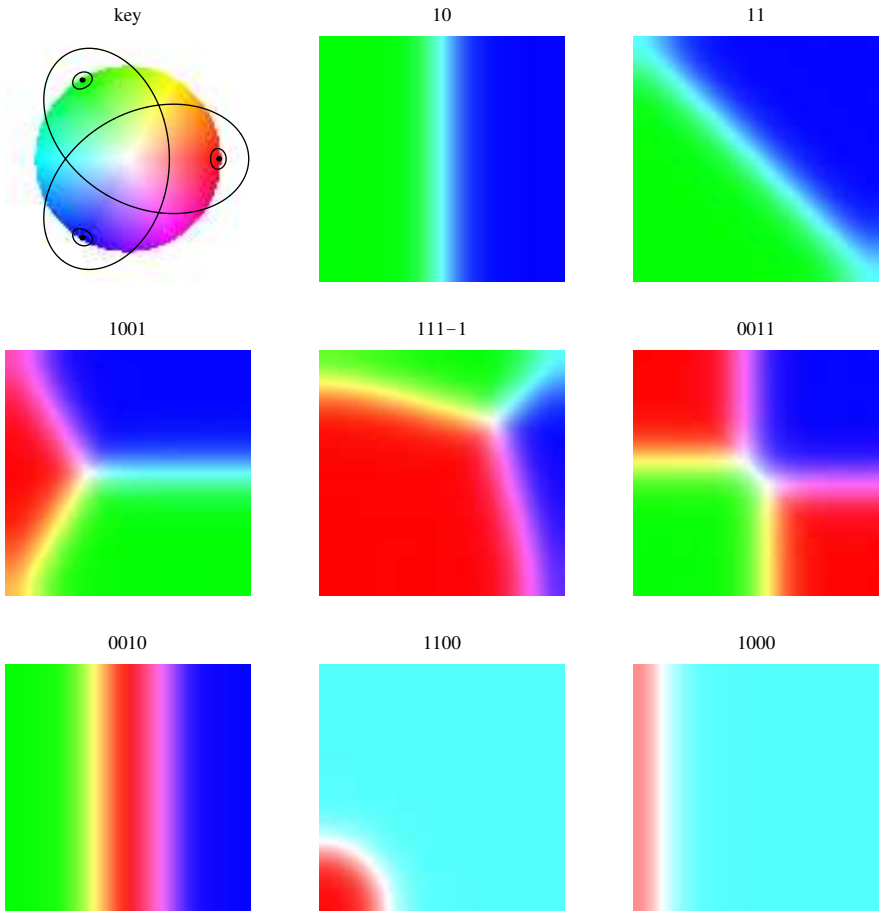

FIGURE 8. All of these solutions are computed at $\epsilon = 0.1$, where the nonlinear corrections to the critical eigenspace are significant. The key at the upper left shows a few contours of the potential W to indicate how the color codes the value of $u(x, y)$. The diagram with the $111-1$ symmetry is the MI 2 triple junction solution which bifurcates off of the maximum trivial branch, as conjectured in [**22**]. See [**39**] for the color version of these graphics which are somewhat more illuminating (used here with permission from the IJBC).

where $W : \mathbf{R}^2 \to \mathbf{R}$ is a C^2 function and $u : \Omega \to \mathbf{R}^2$. Let H be the Sobolev space $H_0^{1,2}(\Omega)$. We want a sufficient hypothesis on W so that the functional $J : H \times H \to \mathbf{R}$ defined by

$$J(u) = \int_\Omega \{\frac{1}{2}|\nabla u|^2 - W(u)\}\, dx$$

has the appropriate properties so that we may mimic the variational arguments found in [CCN]. Corresponding to the hypothesis made on f in [CCN], we may consider assuming that W satisfies the following conditions. Assume that

$$W \text{ has a local minimum } W(0) = 0.$$

Note that this implies that $\nabla W(0) = 0$, which corresponds to $f(0) = 0$. Let $\beta_1 \leq \beta_2$ be the eigenvalues of $D^2W(0)$, which are both positive since W has a local minimum at 0. Assume that

$$\beta_2 < \lambda_1,$$

a condition that parallels the CCN assumption that $f'(0) < \lambda_1$. Corresponding to the CCN convexity assumption $f'(v) > f(v)/v$ for all $|v| \neq 0$, we assume that

$$D^2W(u)u \cdot u > \nabla W(u) \cdot u.$$

The coercivity assumption $\frac{m}{2}vf(v) \geq F(v)$ for some $m \in (0,1)$ where $F(v) = \int_0^v f(s)\,ds$ becomes

$$\frac{m}{2}u \cdot \nabla W(u) \geq W(u),$$

again for some $m \in (0,1)$. In CCN, we required that f be superlinear, i.e., that $f(v)/v \to \infty$ as $|v| \to \infty$. Similarly, for the gradient system one would require that either

$$\frac{|\nabla W(u)|}{|u|} \to \infty \text{ or } \frac{\nabla W(u) \cdot u}{u \cdot u} \to \infty, \text{ as } |u| \to \infty.$$

We are not certain which is the most natural assumption. Both assumptions appear to imply that

$$\frac{W(u)}{u \cdot u} \to \infty \text{ as } |u| \to \infty,$$

where $|u|$ is the Euclidean norm of u in $\mathbf{R}^2$. Finally, we need to assume a subcritical growth of W. One possibility is to assume that there exists $A > 0$ so that

$$D^2W(u)u \cdot u \leq A(|u|^{p-1} + 1)|u|^2.$$

When $N = 2$ this assumption is unnecessary, but for higher N it is required in order for the application of the Sobolev Imbedding Theorem. The "critical hyperboloid" found in the literature suggests that perhaps the above subcritical condition might not be the best possible subcritical assumption.

The question now is whether a CCN-type solution exists to (5.3). If one takes this to mean the existence of a $w = (u, v) \in H \times H$ where both u and v change sign exactly once and w has the smallest J value among all such solutions, then numerical experiments suggest that the solution will be of MI 4 (and hence require 4 constraints for any minimax existence argument). In our research preliminary to the Ginzburg-Landau problem outlined above, we considered systems of scalar equations such as

$$\Delta u + u^3 + cuv = 0, \text{ and } \Delta v + v^3 + cuv = 0.$$

For various reasonable values of the coupling parameter c, we were able to numerically find solutions w where:

(1) w is MI 1, u is of one sign, and v is small.
(2) w is MI 1, v is of one sign, and u is small.
(3) w is MI 2, u and v are of one sign.
(4) w is MI 2, u is small, and v changes sign exactly once.
(5) w is MI 2, v is small, and u changes sign exactly once.
(6) w is MI 3, u is of one sign, and v changes sign exactly once.
(7) w is MI 3, v is of one sign, and u changes sign exactly once.
(8) w is MI 4, u and v change sign exactly once.

Clearly the results from [**8**] confirm the above results when the system is decoupled via setting $c = 0$. It seems reasonable to apply techniques similar to that found in [**8**] to prove the existence of the first three solutions. We are currently unsure as to how to proceed in looking for an existence proof for sign-changing solutions. Note that one could consider the third solution to be a MI 2 sign-changing solution if u and v were one sign solutions of opposite sign.

6. GNGA for General Regions.

We present here a preview of two new results. For general regions, one must first generate a suitable basis for the M dimensional subspace G. In the previous section, we saw an example where, although a basis of eigenfunctions of $-\Delta$ worked, it might not have been the best choice. Here, we are back in the territory of superlinear problems where the linear theory is clearly key in investigating the nonlinear phenomena.

Both experiments use the package ARPACK. At the time of this writing, we are porting both linear and nonlinear code to work in a parallel environment on a Linux cluster. Our scalar processing code uses LAPACK, BLAS, and ARPACK libraries. The parallel code uses MPI together with PARPACK, PBLAS, and SCALAPACK. Once our test platform is upgraded we will be able to repeat experiments with a much higher order of accuracy, as well as perform other experiments such as PDE on high dimensional regions Ω that currently are beyond our computational capabilities.

In [**25**], we consider the case where $\Omega = \Omega_d \subset \mathbf{R}^2$ is a Bunimovich stadion, or so-called billiards table or stadium (see [**6**] and Figure 9). The well-developed linear theory includes such interesting phenomena as crossing eigenvalues and the avoided crossing of eigenvalues. We are able to find many solutions to (1.2), construct bifurcation diagrams using either or both of the parameters $\lambda = f'(0)$ and the stadion dimension d describing the radii of the end caps of Ω_d. We do indeed observe the swapping of symmetry as d passes through a value where an eigenvalue crossing occurs and the corresponding eigenfunctions swap symmetry. The persistence of linear phenomena in nonlinear cases is a theme we return to time and time again. Figure 10 shows the well known symmetry swapping / avoided swapping

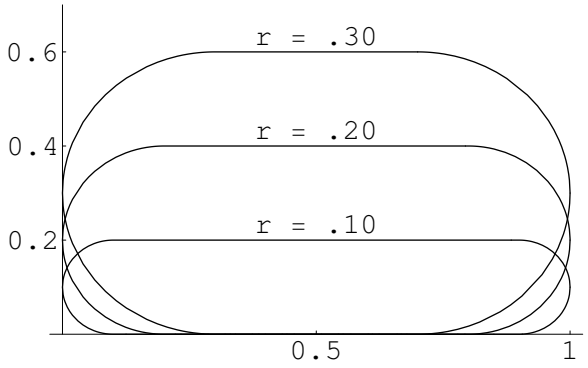

FIGURE 9. A family of Bunimovich stadions, often referred to as billiards or stadiums. Here the length is 1 for each stadium; the represented radii are labeled.

phenomena at a crossing and avoided crossing of eigenvalues. Figure 11 depicts solutions obtained by fixing $\lambda = f'(0)$ at the crossing value and varying the radius parameter d.

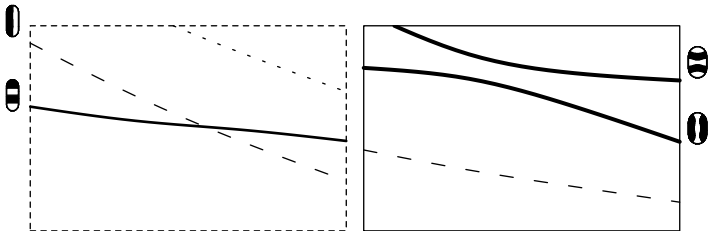

FIGURE 10. The figure on the left depicts the λ_4 and λ_5 crossing as the radius d ranges from $d = .19$ to $d = .21$, along with the accompanying symmetry swapping of ψ_4 and ψ_5. The symmetries are different, that is one branch starts as even in x and odd in y while the other starts as odd in x and even in y; symmetry swapping occurs at the multiple eigenvalue. The figure on the right depicts an avoided crossing of λ_8 and λ_9; the symmetries are the same (even in both variables) and no symmetry swapping occurs. In both graphs a third branch of a different symmetry type is nearby, but has no influence on the symmetry of linear and nonlinear solutions corresponding to the crossing / avoided crossing feature.

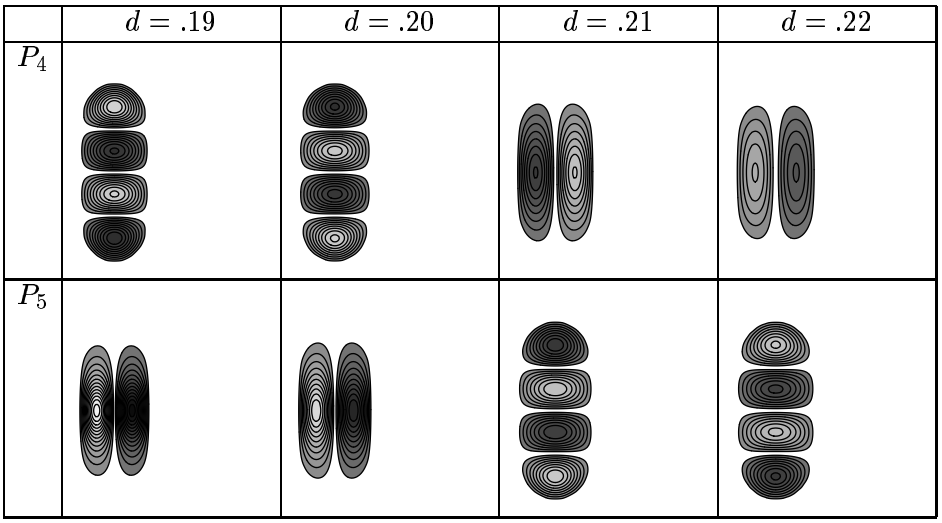

FIGURE 11. Contour plots of solutions on the two branches bifurcating from λ_4 and λ_5. Here, the bifurcation parameter $\lambda = f'(0)$ is held fixed near the multiple crossing eigenvalue and the second parameter d (radii of endcaps) is varied as in the left graphic in Figure 10. The swapping of symmetry for the nonlinear problem is thus evident. Solutions were selected at random from either the initial branch or the negative of that branch; either choice has the same symmetry and nodal structure, differing only by a multiple of -1. The article [**25**] contains more detailed bifurcation diagrams, including secondary bifurcations and deeper symmetry analysis.

We have investigated the case where Ω is the Koch Snowflake. The generation of eigenfunctions required us to essentially repeat the earlier work [**27**]. In our paper, we discuss possible refinements to or at least alternative methods for performing the linear computation. Once a basis was generated, we proceeded as in [**36**], [**7**], and [**25**]. Figure 13 shows a lower level grid approximating the Koch Snowflake. The key to invoking the ARPACK code to calculate eigenvalues of a linear map is in a user provided subroutine wherein the action of the map acting on a vector is coded. For the discretized $-\Delta$ operator and the equilateral grid, this can be easily done. As in Figure 12, let $e_1 = \frac{1}{2}\hat{i} + \frac{\sqrt{3}}{2}\hat{j}$, $e_2 = \hat{i}$, and $e_3 = \frac{1}{2}\hat{i} - \frac{\sqrt{3}}{2}\hat{j}$. Then $u''(x)(e_1, e_1) \approx \frac{a-2o+b}{h^2}$, $u''(x)(e_2, e_2) \approx \frac{c-2o+d}{h^2}$, and $u''(x)(e_3, e_3) \approx \frac{e-2o+f}{h^2}$. Using the bilinearity of $u''(x)$, a simple calculation shows that

$$-\Delta u(x) \approx \frac{2}{3h^2}(6o - (a + b + c + d + e + f)),$$

which is a generalization of the well-known 5-point rectangular second difference formula to this hexagonal situation. Figure 14 contains an example

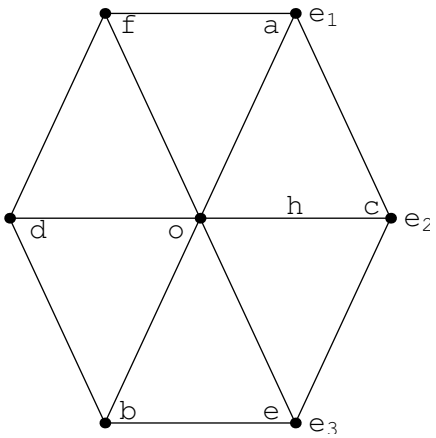

FIGURE 12. A center point x with value o and its 6 neighbors $x \pm he_1$, $x \pm he_2$, and $x \pm he_3$, with values a, b, c, d, e, and f. The gridsize h is proportional to 3^{-k}, where k is the level of the polygonal approximation to the fractal snowflake.

of automated bifurcation branch following output that can be obtained by careful application of the GNGA (see [**38**]). The provided diagram was obtained via repeated calls to an implementation of the GNGA which follows a single branch and saves off initial data for following secondary and tertiary branches when zero eigenvalues of the Hessian $D_2J(u)$ are encountered. Many refinements to our previous branch following methods are possible, for example by using knowledge of the lattice of possible symmetry types obtained by considering isotropy subgroups of the symmetry group of the snowflake $\mathbf{D}_6$ crossed with $\mathbb{Z}_2$ (given our odd choice of nonlinearity). For instance, we can seek only branches of a particular symmetry and/or compute only terms of gradients and Hessians corresponding to a branch's symmetry, hence gaining substantial computational efficiency and some added accuracy. Symmetry information can guide search direction choices at multiple bifurcation points, and be provided as output. Figure 14 contains solutions of 8 symmetry types, among the possible 23 proven to exist in [**38**]. The seven dots on the vertical axis indicate nontrivial solutions of distinct symmetry type; in Figure 15 we present these 7 solutions as well as a solution not found on this particular set of branches, namely a solution with no symmetry (type S_{23} in our notation). The article [**38**] describes in detail the symmetry analysis for this region, the techniques used to invoke the GNGA to perform automated branch following, and a complete graphical description of all solutions to (1.2) on the Koch Snowflake region up to solutions of a moderately high MI. The article [**37**] describes the method used for obtaining the basis of eigenfunctions used in that nonlinear effort via careful usage

of ARPACK, as well as more details concerning our symmetry analysis of the region.

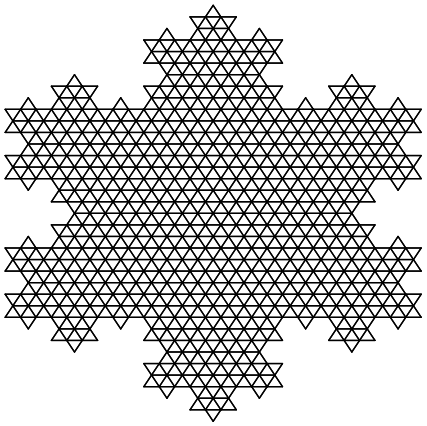

FIGURE 13. Level 3 grid of equilateral triangles used in the ARPACK eigenfunction generation code. We typically use Levels 4 and 5 in our nonlinear experiments and to compare eigenvalues with those previously calculated by [**27**]. Our current basis generation codes use a somewhat modified grid, placing the boundary of the region between grid points and using "ghost points" outside the region to enforce the zero Dirichlet (or Neumann) boundary conditions (see [**37**]).

7. The Lazer-McKenna Conjecture, Dancer Counterexample, Basins of attraction.

The interested reader should consult [**28**], [**29**], [**18**], and references both therein and subsequent by those authors. The issues discussed in these important papers have come to represent to this author the general question of existence and multiplicity of solutions to semilinear elliptic problems. In particular, complete resolutions of the explicit and implied questions within those articles would settle the matter of the conjectured existence of infinitely many solutions to our superlinear problem. Essentially, Lazer and McKenna conjectured that (1.2) should have $2k$ solutions when f had the asymptotically linear form

$$f(u) = \lambda u + g(u) - h_1(x) - s\phi_1,$$

where ϕ_1 is a (normalized) eigenfunction corresponding to the first eigenvalue λ_1, h_1 is orthogonal to ϕ_1 in L_2, s is sufficiently large, and $f \in C^1$ is such that $\limsup_{u\to-\infty}(\lambda u+g(u))/u < \lambda_1$ and $\lambda_k < \lim_{u\to\infty}(\lambda u+g(u))/u < \lambda_{k+1}$. This would prove the existence of arbitrarily many solutions to a subclass of problems of type (1.2), as the number of enclosed eigenvalues increased. However, Dancer proved via a now famous counterexample that

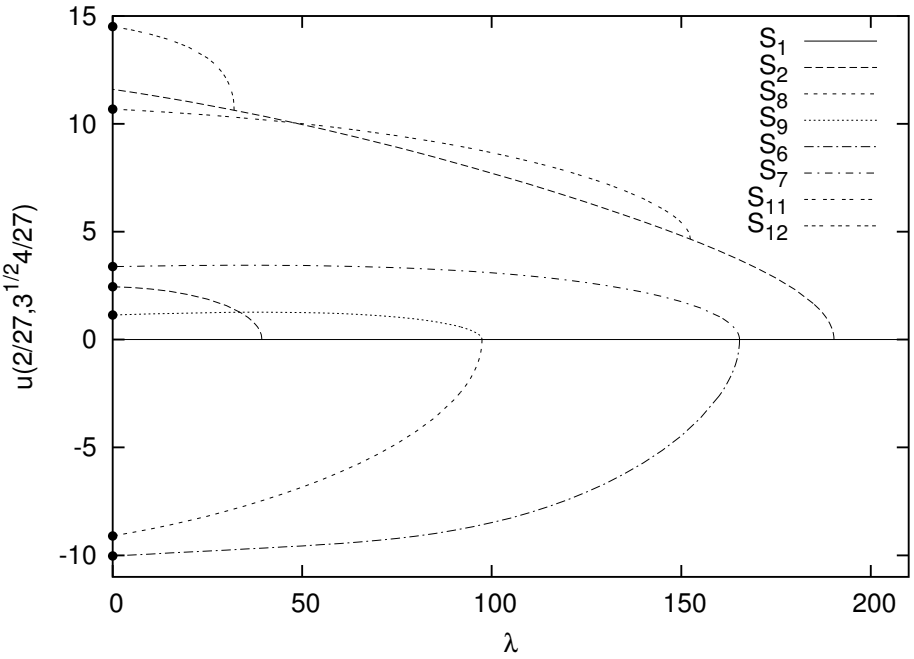

FIGURE 14. Bifurcation diagram for the first four primary branches of (1.2) on the Koch Snowflake. The x-axis is the bifurcation parameter $\lambda = f'(0)$; the y-axis is the value of the solution evaluated at a generic point of the fractal domain, a technique which yields good visual separation of branches. Two secondary bifurcations and 8 of the 23 possible symmetry types are depicted in this graphic. See Figure 15 for contour plots of solutions of the 7 nontrivial symmetry types, that is, not including the zero solution with symmetry type S_1. The fourth primary branch is the second occurrence of symmetry type S_2; its contour plot is also not included. See [**38**] for a complete list of all symmetry types and examples of bifurcation diagrams where each type of solution can be found.

this conjecture is in general false. A key ingredient in the counterexample's construction was the usage of multiple eigenvalues. Assuming that Ω was a ball, $f \in C^\infty$, and that $k+1$ eigenvalues were crossed, Dancer provided an example where only 4 solutions existed for all large s.

This author wishes to state a slightly different conjecture, and to provide a high-level description of some ideas that might be useful in investigating the conjecture's veracity.

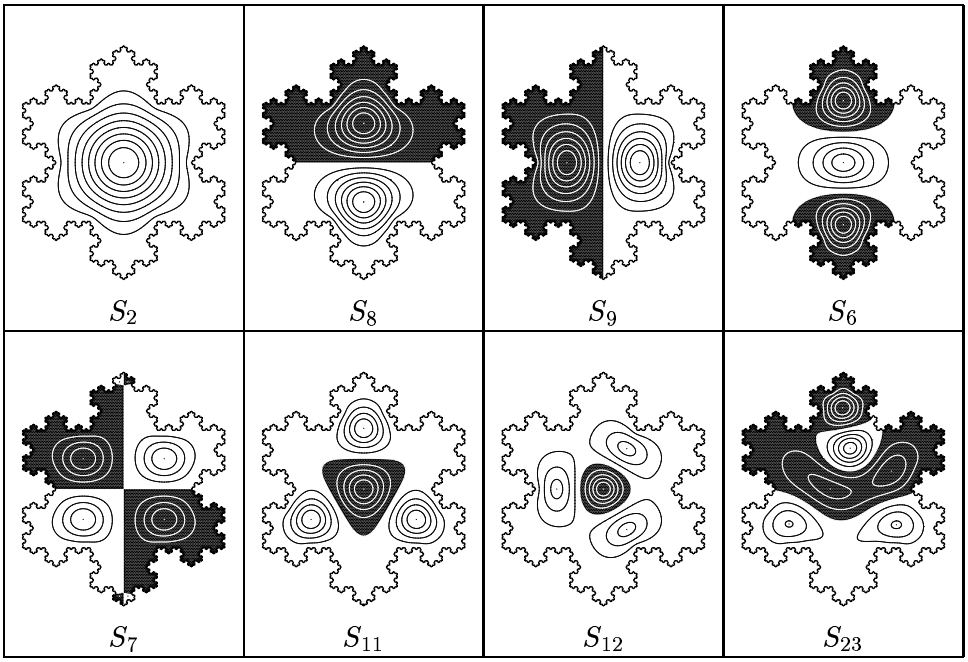

FIGURE 15. Contour plots of solutions corresponding to the 7 nontrivial symmetries found in Figure 14. The third plot is the CCN solution (symmetry type S_9). The eighth plot depicts a non-symmetric solution (symmetry type S_{23}) found on a higher branch.

CONJECTURE 7.1. Let $f \in C^1$ satisfy $f(0) = 0$ and assume that there exists $m \in (0,1)$ such that $\frac{m}{2} f(u)u \geq F(u)$, for $|u| > \rho$, some $\rho > 0$, and that $f'(u) > \frac{f(u)}{u}$ for $u \neq 0$. If the interval (α, β) defined by $\alpha = f'(0) < \lambda_1$ and $\lambda_j < \beta = \lim_{u \to \pm\infty} f(u)/u < \lambda_{j+1}$ contains k *distinct* eigenvalues, then there exist $2k+1$ solutions to (1.2).

Under this hypothesis (see Figure 16), one of these solutions is the trivial solution $u \equiv 0$. It is not difficult to see that the superlinear arguments can be applied to get the 3 nontrivial solutions found in [**2**] and [**8**] even to this asymptotically linear problem, provided that $\beta > \lambda_2$.

One cannot help but gain confidence in the existence of many solutions to (1.2) when observing them numerically using the GNGA. It appears that given a proof of existence of a solution, it should be possible to prove that the GNGA converges to that solution for a suitable initial guess. Conversely, if one could prove that GNGA converged for a given guess, one might be able to conclude analytically that the solution exists. This line of reasoning was the starting point for the Research Experience for Undergraduates (REU) work of Joel Fish (see [**21**]), where we set out to better understand basins

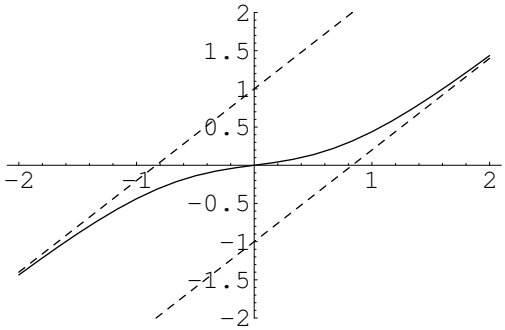

FIGURE 16. Asymptotically linear $f \in C^1$ with $f'(0) = c$, $f'(\pm\infty) = 1 + c \geq 0$ defined by $f(x) = (1+c)x - \tanh x$.

of attraction of continuous Newton's method. To see what is possible, refer to [**43**] for a very simple finite-dimensional example where the basins of attraction are completely understood. A potentially far-reaching analytical result using continuous Newton's method as a tool can be found in [**44**]; therein an elegant result nearly analogous to the celebrated Nash-Mosher theory is proven in a vastly simpler fashion. We must admit up front that the remainder of this section is almost completely conjecture, only marginally supported by numerical evidence. Even if true, the proofs may well be intractable. Never the less, we find that the material suggests intriguing research directions that may well be quite fruitful.

We have observed that the low MI solutions are of simple nodal structure, and thus should have eigenfunction (Fourier) expansions with the first few coefficients dominating. It thus seems reasonable that for sufficiently large $M \in \mathbf{N}$, the $M \times M$ matrix $A = A(u) = (J''(u)(\psi_i, \psi_j))_{i,j=1}^M$ should approximate $D^2J(u)$ well. One can view the approximation as good in the following sense. Firstly, one should have $\mathrm{sig}(D^2J(u)) = \mathrm{sig}(A)$ and that the first few eigenvalues of $D^2J(u)$ and A closely agree. Secondly, the first few eigenvectors of A in $\mathbf{R}^M$, thought of as coordinates in the Galerkin space $G = \mathrm{span}\{\psi_i\}_{i=1}^M$, appear to closely represent the first few eigenfunctions of $D^2J(u)$ in H. If $D^2J(u)$ is invertible this seems provable. It is not clear how to handle the case where the Hessian has one or more zero eigenvalues. Given a nondegenerate solution $v \in H$, we propose that given $\epsilon > 0$ there exist $M \in \mathbf{N}$, $v^* = \sum_{i=1}^M a_i\psi_i \in G = G_M$, and $\delta > 0$ such that $\nabla\hat{J}(a) = 0$, $||v^* - v|| < \epsilon$, and Newton's method (continuous or discrete) converges to $v^* \in G$ given any initial approximation v_0 with $||v^* - v_0|| < \delta$. Experimentally, one uses a small step size to approximate the continuous Newton's flow

$$u'(s) = -(D^2J(u(s)))^{-1}\nabla J(u), \quad u(0) = u_0.$$

Multiplying by $D^2J(u(s))$ and undoing the chain rule results in the initial value problem

$$((\nabla J)(u))'(s) = -\nabla J(u(s)), \quad \nabla J(u(0)) = \nabla J(u_0).$$

The solution is $\nabla J(u(s)) = \nabla J(u_0)e^{-s}$, and so the gradient goes to zero and

$$u'(s) = -(D^2J(u(s)))^{-1}\nabla J(u_0)e^{-s}.$$

If the inverse (pseudoinverse) of $D^2J(u(s))$ could be controlled, then convergence of the flow to a critical point might be proven. The proof that J satisfies the Palais-Smale condition (see [**46**] or [**10**]) or a similar argument might be useful in showing that $\lim_{s\to\infty} u(s)$ exists. The coercivity of J (see [**8**]) might also be appealed to. It seems reasonable that the signature should be constant along these flows, at least when the limit (solution) is nondegenerate. Perhaps the most tractable of our conjectures is that there exist initial values of arbitrarily large signature, whereby convergence along signature-invariant flows would provide the existence of infinitely many solutions.

It is known that the basins of attraction for continuous Newton's method are generally more straightforward than those of discrete Newton's method, typically lacking the fractal boundaries and accompanying dynamical complexities. As in simple cases (where it can be easily proven), continuous Newton's method when applied to the variational formulation of (1.2) appears to have connected basins with measure zero boundary. Obviously if one could describe the basins analytically and if there were infinitely many of them, then one would have the highly desirable result that infinitely many solutions exist.

Together with our Summer 1999 REU student Joel Fish, we have made some progress towards understanding these basins and their boundaries. There are simple examples where continuous Newton flows terminate in finite time to points that are not roots, e.g., where a zero derivative is encountered. The inflection sets (where $D^2J(u(s))$ is not invertible) almost certainly contain such points. The experimental and novel work of our REU student suggests that the collection of initial points that converge to such "bad points" themselves belong to the set

$$\Gamma = \{u \in H : J'(u)(e_i) = 0 \text{ for some eigenfunction } e_i \text{ of } D^2J(u(s))\},$$

which may itself be composed of infinitely many orthogonally intersecting manifolds. It appears to be the case that the inflection sets form part of the boundaries of the basins of attraction for our Newton flows, and that part of Γ forms the rest of the boundaries. Certainly it is clear that all solutions must lie in Γ, possibly at the points where infinitely many (all but one) manifolds intersect orthogonally. Degenerate solutions which belong to both an inflection set and Γ exist and add to the difficulty of finding a proof. Finally, we have experimentally observed a subset of Γ that very closely resembles the manifold S used in CCN in that it appears to be a codimension

1 submanifold diffeomorphic to the unit sphere which contains all nontrivial solutions to (1.2). This very interesting set can be characterized as

$$\Gamma^* = \{u \in H : J'(u)(e_1) = 0, \beta_1 < 0\},$$

where β_1 is the smallest eigenvalue of $D^2J(u)$ and e_1 is the corresponding eigenfunction.

The components of Γ corresponding to a particular eigenfunction e_i (at least locally where unambiguously defined) apparently are both gradient and Newton flow invariant sets. We have a numerical experiment where the one-sign solutions for both the $\Omega = (0,1)$ and $\Omega = (0,1) \times (0,1)$ cases have been found by following such "flows". Specifically, starting with a small guess $c\psi_1$, we iteratively project on to the set $\{u \in H : D^2J(u)\nabla J(u) = \beta_1 \nabla J(u)\}$ and take small gradient steps. This procedure terminates at a one-sign solution approximation where the 1-dimensional set intersects Γ^*. Since $\nabla J(u)$ is parallel to $e_1(u)$ along this set, we sometimes refer to this process as "following the eigenflow". We have had limited success in finding higher MI solutions via this method. For the ODE, the only stumbling block is in the smoothness of the map $e_i = e_i(u)$. It is easy to see that $e_i(0) = \psi_i$, but it does not work to continue to define e_i as the i^{th} eigenfunction of $D^2J(u)$. When a multiplicity is encountered, care is needed to continue in the correct direction, often requiring a reordering of the eigenvalues of $D^2J(u)$. For the PDE, the matter is even more complicated. Our experiments on the unit square have so far failed to work for all but the MI 1 solutions, likely due to the multiplicity of the 2nd eigenvalue.

We believe that eigenflows corresponding to distinct simple eigenvalues λ_i should converge to one of two solutions, corresponding to the directions $\pm\psi_i = \pm e_i(0)$. This contributes $2p$ solutions towards the conjectured $2k+1$, for the p simple eigenvalues found among the k distinct eigenvalues in $\lambda_1 < \lambda_2 \leq \cdots \leq \lambda_j < \lambda_{j+1}$. The other $2(k-p)$ solutions are much more complicated to understand. Ironically, in most of the situations that we have encountered multiplicity leads to a proliferation of solutions of all possible symmetries, rather than leading to nonexistence. For an eigenvalue λ_i of multiplicity $r > 1$, we envision an r-dimensional eigenflow-invariant manifold emanating from the origin, intersecting the S-like set Γ^* in a $r-1$ dimensional submanifold. The 2 solutions contributed by this distinct eigenvalue would be a minimizer and maximizer of J restricted to this submanifold of Γ^*. We have some numerical evidence that a solution corresponding to a eigenfunction ψ_i will have a MI in the range $\{i, \ldots, i+r+s\}$, where r and s are the multiplicities of λ_i and the next distinct eigenvalue, respectively.

8. Open Problems and Future Directions.

We now present open problems requiring analytical investigation, feasible new numerical experiments, and new ideas that merit further study. We proceed with the former:

A1 **Zero-Set Conjecture.** All of our numerical experiments support the conjecture that the CCN solution to the superlinear problem has an internal zero set which intersects the boundary $\partial\Omega$. In particular, if proven this would imply that the MI 2 CCN solution on the ball is non-radial. When $\Omega = (0,1) \times (0,1)$, the solution possessing 90^o rotationally invariant symmetry (where the zero-set is a closed loop in Ω) is the one corresponding to $\psi_{1,3} + \psi_{3,1}$ (see [**17**] and [**36**]). Our numerical experiment provides a MI greater than 2, supporting that this is not the CCN solution. A starting point for proving this conjecture is the theorem by Melas (see [**32**]) where it is proven that if Ω is a bounded and convex region in $\mathbf{R}^2$, then the second eigenfunction ψ_2 has this property, i.e., its internal zero set intersects the boundary in exactly two points. A related question is whether or not the zero-set is connected. The author feels that geometric arguments similar to the "Moving Planes" of [**23**] may be the key (albeit some sign-changing variant).

A2 **The Second CCN Solution.** As a first step towards finding more solutions to our superlinear problem, one could try to find a second CCN solution. This solution roughly corresponds to the negative of the solution already proven to exist. As in the "8 solutions on the square" problem below, one would generally expect more solutions depending on the symmetry of the region Ω. Finding this solution might be very important, as a linking or mountain pass argument restricted to S_1 (see (2.7)) might then lead to a higher energy MI 3 solution. Potentially, if that argument in turn was useful in obtaining a second MI 3 solution, there might be a snowball effect whereby infinitely many solutions could be found.

A3 **Infinitely Many Solutions.** It is widely (but not universally) believed that the superlinear problem has infinitely many solutions. This is the logical extension to the facts that there are indeed infinitely many solutions when $\Omega \subset \mathbf{R}$, Ω is a ball in $\mathbf{R}^N$, or when f is odd. We find that a series of papers by Lazer-McKenna and Dancer is essential reading when considering this open question (see for example [**18**] and [**28**], and Section 7 above.) This problem's difficulty is confirmed by the more than half a century of sustained effort mathematicians have exerted since Ljusternik and Schnirrleman's celebrated "f odd" result. Ambrosetti, Castro, Costa, Dancer, and Rabinowitz, to name just a few involved in this effort, have all given the problem considerable thought. Item C1 below suggests a possible research direction to follow in considering this problem.

A4 **Sublinear Dirichlet Problem.** When the nonlinearity f is taken to be sublinear, the hypothesis of Theorem 2.1 can be restated in a natural way. For example, $f(0) = 0$, $f'(0) > \lambda_k$, $\frac{f(u)}{u} \to 0$ as

$|u| \to \infty$, $\frac{m}{2}uf(u) \leq F(u)$, and $f'(u) < \frac{f(u)}{u}$ for $u \neq 0$. Our numerical experiments suggest that a sign-changing exactly-once solution analogous to the CCN solution persists. Like the situation in [**11**], the Nehari manifold is degenerate at 0. Different techniques must be used. It may be that the Lyapunov-Schmidt reduction method will again prove useful.

A5 **Eight Solutions on the Unit Square.** In many of our numerical experiments it has become obvious how to completely classify certain low energy, low MI solutions. For example, when $\Omega = (0,1) \times (0,1)$, one might prove the existence of the 8 sign-changing exactly-once solutions (4 MI 2 CCN solutions and 4 MI 3 solutions) depicted on the 2nd and 3rd branches bifurcating at $\lambda_{12} = \lambda_{21} = 5\pi^2$ in Figure 2. Note that if f is odd, then one can "stitch together" one-sign solutions on subregions and tile patterns to get these solutions and many more.

A6 **Is S_1 a Manifold?** If not, how and where does it fail? If S_1 (see (2.7)) were a manifold, the existence proof found in [**8**] could be considerably simplified. It appears that the lack of differentiability of the map $u \to u_+$ plays a role here. A related but easier question is whether or not S_1 is connected; we conjecture that this is so.

A7 **Convergence of GNGA.** It should be possible (for at least some special cases) to prove that given a solution ω to (1.2) and $\epsilon > 0$ that there exists a natural number M and a real number $\delta > 0$ so that if $||\omega - u_0|| < \delta$, $u_0 \in G = \text{span}\{\psi_1, \ldots, \psi_M\}$, then the GNGA with the initial guess u_0 will converge to a function $\hat{\omega} \in G$ with $||\omega - \hat{\omega}|| < \epsilon$. A starting point for proving this might be found in [**19**] and references both subsequent and therein. Using their theory, it seems reasonable that one could prove that given $u \in G$, a natural number k, and a real number $\epsilon > 0$, there exists M sufficiently large so that the first k eigenvalues of the $M \times M$ Hessian approximation matrix A from (2.1) will be within ϵ of the first k eigenvalues of the true Hessian $D_2^2 J(u)$. This problem is likely very difficult, although partial results may be more tractable.

The author hopes that the above problems have been stated precisely enough so that the interested researcher could begin or resume thinking about them immediately. The following list contains suggested numerical experiments for the future. All of them could be investigated using the GNGA; indeed some of them have already been partially attempted.

B1 **Higher Dimensional Regions for GNGA.** There is no reason that one cannot implement GNGA for $\Omega \subset \mathbf{R}^N$, $N > 2$. The difficulties are largely related to efficiency and accuracy. ARPACK will handle the eigenbasis generation on arbitrary regions, given proper computational power. It may be that Monte-Carlo techniques will be useful when performing numerical integration in calculating the

gradient and Hessian. Some thought has been given to perhaps generating a random grid, where the vertices provide the Monte-Carlo points and the graph (irregular grid) could be used by ARPACK to approximate eigenfunctions.

B2 **More General Region Experiments.** Using generic eigenfunction generating code (such as ARPACK) for arbitrary regions in the plane (or indeed in higher dimensions), we can continue to repeat our nonlinear experiments for other interesting shapes, such as dumb-bells, where the eigenfunctions may not be known in closed form. One hopes that the effects of the choice of Ω on the bifurcation diagrams will continue to be enlightening. A region that interests the author and may present implementational challenges is the Mandlebrot set. In general, one wonders how much effect fractal boundaries have on solutions to (1.2). For example, in the Koch Snowflake experiments, would the most interesting phenomena be captured by studying the far simpler hexagon region with apparently the same symmetries?

B3 **Fucik Spectrum and GNGA.** There is every reason to believe that numerical experiments for nonlinearities of the form $f(u) = au_+ - bu_-$ will be effective in shedding light on many open problems concerning Fucik spectrum.

B4 **Secondary Bifurcations for Superlinear Problems on the Disk.** Our initial experiments are inconclusive. It should be fairly straightforward to determine numerically if there is or is not secondary bifurcation analogous to that found in [**36**] when Ω is a disk in $\mathbf{R}^2$.

B5 **Alternate Basis for GNGA.** For our superlinear problem, it seems clear that eigenfunctions of the Laplacian are the natural choice. For other problems, such as the Ginzburg-Landau equation in [**39**], this may not be the case. Whenever solutions tend towards step functions, have "vortices", or other more pathological features, Fourier expansions leave something to be desired. We presented in Section 2 a trivial example where Legendre polynomials were used. Among other possibilities, wavelet and frame theory may suggest suitable alternatives.

B6 **Full Ginzburg-Landau Application of GNGA.** In [**42**] the functional for this substantially difficult problem is given:

(8.1)
$$E(u,A) = \int_\Omega \left(\frac{1}{2}|(\nabla - iA)u|^2 + \frac{1}{2}|\nabla \times A - H_0|^2 + \frac{\kappa^2}{4}((1-|u|^2)^2 \right) dx,$$

The region Ω is a subset of $\mathbf{R}^p$, for $p = 2$ or $p = 3$. Here the unknowns are the order parameter $u \in H^{1,2}(\Omega, \mathbf{C})$ and the vector potential $A \in H^{1,2}(\Omega, \mathbf{R}^p)$. If the applied magnetic field H_0 is identically zero, then we can assume that $A(x) = 0$ and the

Euler-Lagrange equation of (8.1) reduces to (5.1), where $\kappa = 1/\epsilon$. One challenge that presents itself in investigating this problem is in dealing with the natural boundary conditions

$$(\nabla \times A) \times \eta = H_0 \times \eta \text{ and } ((\nabla - iA)u) \cdot \eta = 0,$$

where η is as before the outward unit normal. There is a great body of literature considering various facets of the analysis of Ginzburg-Landau problems, of which we have referenced only a few select works. References to numerical investigations of these problems are somewhat sparse. Very little can be found concerning analysis or numerics in the "full Ginzburg-Landau" case. We find that GNGA using some suitable basis should be an effective tool for investigating this important equation, as a similar but competitor technique to those found in [**42**]. The same comment applies to the following problem.

B7 **Monge-Ampere Application of GNGA.** We can find almost no literature concerning the numerical investigation of the Monge-Ampere equation $|D^2u| = f(x,u)$ on $\Omega \subset \mathbf{R}^N$ (with suitable boundary conditions). Indeed, there appears to be almost no analytical work in cases where the choice of f leads to sign-changing solutions and the principal part becomes in places non-elliptic. We have successfully performed preliminary GNGA experiments on this equation, for simple examples such as the case $\Omega = (0,1) \times (0,1)$, with zero-Dirichlet boundary conditions, $f \equiv 1$, while seeking only negative solutions.

B8 **Nonlinear Partial Difference Equations (PdE) on Graphs.** The Laplacian operator L can be defined and has been well studied on graphs $G = (V,E)$ with $m = |V|$ and $n = |E|$ finite (see for example [**5**]). When the graph is a regular grid, it can be shown that this linear operator converges to the usual Laplacian (with zero Neumann boundary conditions) as the mesh goes to zero. In [**40**], we seek solutions $u : V \to \mathbf{R}$, identified with vectors $u \in \mathbf{R}^m$, to the semilinear elliptic partial difference equation (PdE)

$$-Lu + f(u) = 0$$

on the graph G. Using a variational approach entirely analogous to that used when studying the PDE (1.2), we successfully investigated the PdE by finding critical points of the functional $J : \mathbf{R}^m \to \mathbf{R}$ defined by

$$J(u) = \frac{1}{2} Du \cdot Du - \sum_{i=1}^{m} F(u_i),$$

where $F' = f$. In [**40**] and following [**8**] and [**17**], we are able to prove the existence of one-sign and sign-changing solutions and to prove the existence of solutions with symmetry. Additionally and

following [**34**] and [**15**], we apply variants of the MPA and MMPA to approximate low MI solutions numerically. Following [**36**], we also apply a version of the GNGA suitably adapted for PdE to plot bifurcation curves and provide MI, symmetry, and nodal structure information.

In the spirit of our most recent works [**37**] and [**38**], it remains to modify the ARPACK basis generating code to compute bases for large graphs, analyze the symmetry of the resulting eigenfunctions, apply our automated branch following techniques, and further analyze and exploit the lattice of symmetries for the nonlinear PdE. This project appears to be as open-ended as the subject of graph theory itself.

B9 **Parallel implementation of GNGA.** Larger problems and more details may be handled by first using PARPACK, the parallel version of ARPACK, to generate bases of eigenfunctions. One could use SCALAPACK or other parallel libraries of matrix routines to port the GNGA to this environment, but we are suggesting a simpler scheme. Namely, it seems efficient to have scalar routines implement the following of a single branch on each node, concurrently, and then rely on a master script on the main node to farm out new branch following jobs for secondary and tertiary branches as the need to do so occurs. In this way, our methodology and implementation from [**38**] hardly changes; we just follow one branch per node at the same time rather than proceed through the growing list of branches sequentially.

The above problems can be attempted immediately with GNGA, although additional analytical insight might be required in picking appropriate bases and initial guesses. The following problems are less well defined, representing only suggested future research directions.

C1 **Following Eigenflows.** Since our interest is primarily in proving existence theorems in elliptic PDE, we are hopeful that GNGA will be useful in providing insight (such as the MI of solutions) and may be of direct use in proving such theorems by analyzing continuous Newton flows. The algorithm suggested in Section 7 for following "eigenflows" needs to be refined and more carefully studied, particularly for the PDE and multiple eigenvalues.

C2 **CCN Solutions for Systems.** It seems reasonable to prove the existence of sign-changing solutions to elliptic semilinear problems for systems. The variational structure is clearly more complicated than in the scalar case. In particular, the pseudo-linearity of the maps $u \to u_{\pm}$ used in [**8**] in conjunction with the separating property of S_1 does not appear to persist. Experiments show that a solution $u = (u_1, u_2)$ where both u_1 and u_2 change sign exactly once should be of MI 4, necessitating more constraints. There is a

good, fairly well defined problem to solve here. See the ending note in Section 5 for a precise statement of one possible hypothesis to consider when looking for a CCN solution to a superlinear system, as well as a brief report of an unpublished numerical experiment.

C3 **Semilinear Parabolic Problems.** It should be possible to apply what we now know and what we conjecture for semilinear elliptic problems to the non-steady state case. For example, can we find and understand an unstable flow where the time slices are CCN solutions to elliptic problems? We have extended the idea of PdE (see item B8 above) to heat equations. Will it be fruitful to further develop this to nonlinear parabolic PdE? Can pattern formation and symmetry be explored in a new way in this setting?

9. Conclusion.

GNGA can be an effective tool for investigating nonlinear phenomena. One needs a natural variational formulation, a suitable basis, and some intuition guiding the choosing of initial guesses. The technique seems particularly well suited to semilinear elliptic problems, where one expects a high degree of interaction with the linear problem whose solutions constitute the basis. Thus, for these types of problems we have all three essential ingredients in order to apply GNGA. Tongue in cheek, we like to think of the method as "counter constructive", i.e., it may at times suggest existence proofs just as a constructive proof suggests an algorithm. We believe that eventually, and with possibly great effort, consideration of the basins of attraction for continuous Newton's method as applied to finding critical points of variational functionals for semilinear elliptic PDE will lead to progress towards solving many of the subject's open questions.

References

[1] Adams, R., *Sobolev Spaces*, Academic Press: New York (1975).

[2] Ambrosetti, A.; Rabinowitz, P. *Dual variational methods in critical point theory and applications.*, J. Functional Analysis **14** (1973), p349-381.

[3] Argyros, I., *The Asymptotic Mesh Independence Principal for Inexact Newton-Galerkin-Like Methods*, Preprint (1999).

[4] Aubin, T., *Nonlinear analysis on manifolds. Monge-Ampre equations*, Grundlehren der Mathematischen Wissenschaften [Fundamental Principles of Mathematical Sciences], **252**, Springer-Verlag, New York, (1982).

[5] Bapat, R. B., *The Laplacian matrix of a graph*, Math. Student **65** (1996), no. 1-4, p214-223.

[6] Bunimovich, L. A., *On the ergodic properties of nowhere dispersing billiards*, Comm. Math. Phys. **65** (1979), no. 3, p295-312.

[7] Michael Butros, *Newton's method for semilinear BVP on the disk*, M.S. Thesis (2000), Northern Arizona University.

[8] Castro, A.; Cossio, J.; Neuberger, John M., *Sign-Changing Solutions for a Superlinear Dirichlet Problem*, **27** (1997), no. 4, p1041-1053.

[9] Castro, A.; Cossio, J.; Neuberger, John M., *On Multiple Solutions of a Nonlinear Dirichlet Problem*, Proceedings of the Second World Congress of Nonlinear Analysts, Part 6 (Athens, 1996). Nonlinear Anal. **30**, no. 6 (1997), p3657–3662.

[10] Castro, A.; Cossio, J.; Neuberger, John M., *A Minmax Principle, Index of the Critical Point, and Existence of Sign-Changing Solutions to Elliptic Boundary Value Problems*, Electron. J. Differential Equations, No. 02 (1998), 18 pp.

[11] Castro, A.; Drabek, P.; Neuberger, John M., *Sign-Changing Solutions for a Superlinear Dirichlet Problem, II*, Proceedings of the Fifth Mississippi State Conference on Differential Equations and Computational Simulations, EJDE **10** (2003).

[12] Castro, A.; Kurepa, A., *Infinitely many radially symmetric solutions to a superlinear Dirichlet problem in a Ball*, Proc. of the AMS **101** (1987), p57-64.

[13] Choi, Y. S.; McKenna, P. J., *A Mountain Pass Method for the Numerical Solutions of Semilinear Elliptic Problems*, Nonlinear Analysis, **20** (1993), p417-437.

[14] Chow, S. N.; Hale, J. K., *Methods of Bifurcation Theory*, Springer-Verlag - Berlin, New York (1982).

[15] *A Numerical Reduction Method for Investigating Semilinear Elliptic PDE*, Proceedings of the Second World Congress of Nonlinear Analysts, (Catania, 2000). Nonlinear Anal. **47**, p3379-3390.

[16] Ding, Z.; Costa, D.; Chen, G., *A high-linking algorithm for sign-changing solutions of semilinear elliptic equations.*, Nonlinear Anal. **38** (1999), no. 2, Ser. A: Theory Methods, p151-172.

[17] Costa, D.; Ding, Z.; Neuberger, John M., *A Numerical Investigation of Sign-Changing Solutions to Superlinear Elliptic Equations on Symmetric Domains*, J. Comput. Appl. Math. **131** (2001), no. 1-2, p299-319.

[18] Dancer, E. N., *A counterexample to the Lazer-McKenna conjecture*, Nonlinear Anal. **13** (1989), no. 1, p19-21.

[19] Descloux, J.; Nassif, N.; Rappaz, J., *On spectral approximation. I. The problem of convergence*, RAIRO Anal. Numr. **12** (1978), no. 2, p97-112, iii.

[20] Kinderlehrer, D.; Stampacchia, G., *Introduction to Variational Inequalities and Their Applications*, Academic Press : New York (1979).

[21] Fish, J.; Neuberger, John M., *Eigenflows and basins of attraction for Newton's method*, unpublished REU report (2000).

[22] Flores, G.; Padilla, P.; Tonegawa, Y., *Higher energy solutions in the theory of phase transitions: a variational approach*, Special issue in celebration of Jack K. Hale's 70th birthday, Part 3 (Atlanta, GA/Lisbon, 1998), J. Differential Equations **169** (2001), no. 1, p190-207.

[23] Gidas, B.; Ni, W. M.; Nirenberg, L. *Symmetry of positive solutions of nonlinear elliptic equations in R^n*, Mathematical analysis and applications, Part A, Adv. in Math. Suppl. Stud., 7a, Academic Press, New York-London, (1981), p369-402.

[24] Gilbarg, D; Trudinger, N., *Elliptic Partial Differential Equations of Second Order*, Springer-Verlag: Berlin, New York (1983).

[25] Hineman, J.; Neuberger, John M.; Swift, James W., *Numerical Solutions to Semilinear Elliptic BVP on Bunimovich Stadia*, Work in Progress.

[26] Johnson, L.; Riess, R., *Numerical Analysis*, Addison-Wesley : Reading, Mass. (1982).

[27] Lapidus, M.; Neuberger, J. W.; Renka, R.; Griffith, C., *Snowflake harmonics and computer graphics: numerical computation of spectra on fractal drums*, Internat. J. Bifur. Chaos Appl. Sci. Engrg. **6** (1996), no. 7, p1185-1210.

[28] Lazer, A. C.; McKenna, P. J. *On the number of solutions of a nonlinear Dirichlet problem.*, J. Math. Anal. Appl. **84** (1981), no. 1, p282-294.

[29] Lazer, A. C.; McKenna, P. J., *On a conjecture related to the number of solutions of a nonlinear Dirichlet problem*, Proc. Roy. Soc. Edinburgh Sect. A **95** (1983), no. 3-4, p275-283.

[30] Ljusternik , L.; Schnirrelmann, L., *Methodes Topologique dans les Problems Variational*, Hermann and Cie, Paris (1934).

[31] Z. Mei, *Numerical bifurcation analysis for reaction-diffusion equations*, Springer Series in Computational Mathematics, **28**. Springer-Verlag, Berlin (2000), xiv+414 pp.

[32] Melas, A., *On the nodal line of the second eigenfunction of the Laplacian in R^2*, J. Differential Geom. **35** (1992), no. 1, p255-263.

[33] Milnor, J., *Morse Theory*, Princeton University Press : Princeton (1963).

[34] Neuberger, John M., *A Numerical Method for Finding Sign-Changing Solutions of Superlinear Dirichlet Problems*, Nonlinear World **4**, no. 1 (1997), p73-83.

[35] Neuberger, John M., *A Sign-Changing Solution for a Superlinear Dirichlet Problem with a Reaction Term Nonzero at Zero*, Nonlinear Anal. **33**, no. 5 (1998), p427-441.

[36] Neuberger, John M.; Swift, James W. , *Newton's method and Morse index for semilinear elliptic PDEs*, Internat. J. Bifur. Chaos Appl. Sci. Engrg. **11** (2001), no. 3, p801-820.

[37] Neuberger, John M.; Sieben, N.; Swift, James W., *Computing Eigenfunctions on the Koch Snowflake: A New Grid and Symmetry*, submitted for publication (2004).

[38] Neuberger, John M.; Sieben, N.; Swift, James W., *A semilinear elliptic PDE on a Fractal Domain*, Work in Progress (2004).

[39] Neuberger, John M.; Rice, Dennis; Swift, James W. , *Numerical Solutions to a Vector Ginzburg-Landau Equation with Triple-Well Potential*, Int. J. Biff. Chaos. **13**, No. 11 (2003) p3295-3306.

[40] Neuberger, John M., *Nonlinear Elliptic Partial Difference Equations on Graphs*, preprint, submitted (2003).

[41] Neuberger, J. W., *Constructive Variational Methods for Differential Equations*, Numerical Analysis, Theory, Methods, and Applications, **13**, no. 4 (1988), p413-428.

[42] Neuberger, J. W., *Sobolev Gradients and Differential Equations*, Springer Lecture Notes, (1997).

[43] Neuberger, J. W., *Continuous Newton's method for polynomials*, Math. Intelligencer **21** (1999), no. 3, p18-23.

[44] Neuberger, J. W., *A Nash-Moser theorem with near-minimal hypothesis*, Int. J. Pure Appl. Math. **4** (2003), no. 3, p269-280.

[45] Neuberger, B.; Neuberger, J. W.; Noid, D. W., *Eigenfunctions on a Stadium Associated with Avoided Crossings of Energy Levels*, http://arxiv.org/abs/math.NA/0105217 (2001).

[46] Rabinowitz, P., *Minimax Methods in Critical Point Theory with Applications to Differential Equations*, Regional Conference Series in Mathematics, **65**, AMS : Providence, R.I. (1986).

[47] Tehrani, H., *H^1 versus C^1 local minimizers on manifolds*, Nonlinear Anal. **26**, no. 9 (1996), p1491-1509.

[48] Wang, Z. Q., *On a Superlinear Elliptic Equation*, Ann. Inst. H. Poincare Analyse Non Lineaire **8** (1991), p43-57.

Department of Mathematics and Statistics, Northern Arizona University
PO Box 5717, Flagstaff, AZ 86011-5717, USA
E-mail address: John.Neuberger@nau.edu